FEDERAL UNIVERSITY OF ESPIRITO SANTO
TECHNOLOGICAL CENTER
GRADUATE PROGRAM IN ELECTRICAL ENGINEERING

ALAN SILVA DA PAZ FLORIANO

Brain-Computer Interface Based on High-Frequency Steady-State Visual Evoked Potentials from Below-the-Hairline Areas

Vitória, Brazil

2019

ALAN SILVA DA PAZ FLORIANO

Brain-Computer Interface Based on High-Frequency Steady-State Visual Evoked Potentials from Below-the-Hairline Areas

Thesis presented to the Graduate Program in Electrical Engineering at the Federal University of Espirito Santo, as a partial requirement for the degree of Doctor in Electrical Engineering.

Federal University of Espírito Santo – UFES

Technological Center

Graduate Program in Electrical Engineering

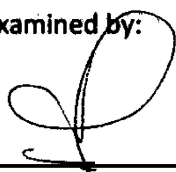Supervisor: Dr. Teodiano Freire Bastos Filho

Vitória, Brazil

2019

ALAN SILVA DA PAZ FLORIANO

Brain-Computer Interface Based on High-Frequency Steady-State Visual Evoked Potentials from Below-the-Hairline Areas
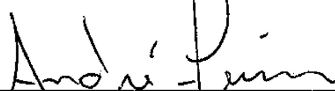
Thesis presented to the Graduate Program in Electrical Engineering at the Federal University of Espirito Santo, as a partial requirement for the degree of Doctor in Electrical Engineering.
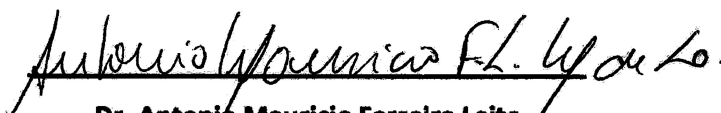
Presented on June 19, 2019. Examined by:

Dr. Teodiano Freire Bastos Filho
(UFES/Brazil)
Supervisor

Dr. André Ferreira
(UFES/Brazil)
Jury

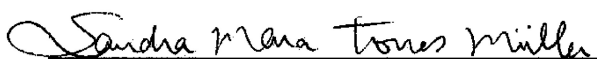---
Dr. Antonio Mauricio Ferreira Leite Miranda de Sá
(UFRJ/Brazil)
Jury

Dr. Pablo Federico Diez
(UNSJ/Argentina)
Jury

Dr. Sandra Mara Torres Müller
(IFES/Brazil)
Jury

To my family, for their unconditional love.

Acknowledgements

I would like to thank my supervisor, Prof. Teodiano Bastos, for the patient guidance, encouragement and advice he has provided throughout my time as his student.

Also, I would like to express my thanks to Dr. Pablo F. Diez, Victor Luciano Carmona and other colleagues of GATEME Lab who supported me during my stay in San Juan/Argentina.

I am also grateful to Prof. Dr. Sridhar Krishnan, Alice Rueda, Dharmendra Gurve, Michael Zara (SAR Lab/Ryerson University) who supported me during my stay in Toronto/Canada.

I want to thank the CAPES/Brazil for my scholarship and for financing the research project - (process 88887.095636/2015-01).

I want to thank Denis Delisle, Javier Castillo, Berthil Longo, Laura Vargas, Viviane Cardoso, Nicolás Valencia, Yves Coelho, Alexandre Bissoli, Carlos Valadão, Eduardo Montenegro, Christiane Goulart, Cecilia Parra, Flavia Loterio, Alexandre Pomer-Escher, Kevin Hernández Ossa, Alejandra Laiseca, John Villarejo, Leandro Bueno, Mario Jiménez, Mariana Midori, Francisco Santos, Andrés Ramirez, Anibal Cotrina, Juan Fernando, Eliete Caldeira, which I met at NTA/UFES, who helped me directly or indirectly in my personal formation and professional.

Finally, I am grateful to my family, who is the emotional support of my life and who is always with me, despite the distance, in the decisive moments of my life.

The compass of science is the human imagination.

The author.

Abstract

Steady-State Visual Evoked Potentials (SSVEPs) are brain responses that present the same frequency (and/or harmonics) of the visual stimulation. Applications, such as Brain-Computer Interfaces, can be derived of their properties. SSVEP response is often maximal on the visual cortex area, consequently, most of the existing SSVEP-based BCIs use electrodes located at occipital and parietal regions. However, these areas are generally covered by hair, which cause complications in the electrode contact with the skin. On the other hand, currently, researchers are looking at how to transfer BCIs from the lab to the patient's home. Recent studies have reported the use of below-the-hairline areas, such as behind-the-ears (temporal area), with stimuli in low/medium frequency bands, to control BCI systems, which suggests that measuring the EEG from hairless areas presents key advantages for technology transfer. However, the visual stimuli in low/medium frequencies used in these studies can produce visual fatigue and other problems to users. This thesis presents studies about characterization of SSVEP response from below-the-hairline areas in high-frequency, with the aim of developing a practical BCI without generating discomfort to users. First, results of our research indicate that SSVEP response from hairless areas are influenced by the reference electrode position, and that the best configuration to measure this response is temporal-frontal montage (TP9-Fpz and TP10-Fpz). The second important result found in our research was that chromatic and luminance stimuli elicit strong SSVEP on the hairless areas, and that the SSVEP response is related to frequency and stimuli color. Results indicate that green-red stimulus elicits the highest SSVEP response in the medium-frequency range (15-25 Hz). On the other hand, green-blue stimulus elicits the highest SSVEP at high-frequencies (30-40 Hz). In addiction, results show that a combination of colors and luminance enhance the SSVEP detection accuracy. Another important contribution of our research was the combination of high-frequency SSVEP (from below-the-hairline areas) with eye focusing mechanism (Depth-of-Field) to command a robot in a virtual environment. In online tests, the volunteers achieved an success rate of 96%. These findings contribute to state of the art, and the development of more practical and comfortable BCIs.

Key-words: BCI, SSVEP, EEG, Below-the-hairline areas.

List of Figures

List of Tables

List of abbreviations and acronyms

BCI   Brain–Computer Interface

CCA   Canonical Correlation Analysis

CRT   Cathodic Ray Tube

EEG   Electroencephalography

ERD   Event Related Desynchronization

ERS   Event Related Synchronization

FBCCA   Filter Bank Canonical Correlation Analysis

FFT   Fast Fourier Transform

fMRI   Functional Magnetic Resonance Imaging

ITR   Information Transfer Rate

LCD   Liquid Crystal Display

LED   Light Emitting Diode

MEG   Magnetoencephalography

MSI   Multivariate Synchronization Index

PET   Positron Emission Tomography

PSDA   Power Spectral Density Analysis

SCP   Slow Cortical Potential

SSVEP   Steady-State Visual Evoked Potential

TMSI   Temporally Local Multivariate Synchronization Index

List of symbols

α 8–13 Hz.

β 13–30 Hz.

δ 0.5–4 Hz.

γ 30–100 Hz.

θ 4–8 Hz.

Contents

1 Introduction

A portion of the population is composed of people affected by severe health problems, such as brain stem stroke, spinal cord injury, Amyotrophic Lateral Sclerosis (ALS) and muscular dystrophies. Because of these problems, interfaces that use speech or limbs movements become hard to be utilized. Biological signals are a key factor in development of non-conventional channels of communication between humans and machines. The development of several assistive technologies (AT) explores these novel interaction links (NICOLAS-ALONSO; GOMEZ-GIL, 2012). In this scenario, Brain-Computer Interfaces (BCIs) play an important role, as they allow extracting information from brain signals, relating them with commands into an application (NICOLAS-ALONSO; GOMEZ-GIL, 2012). Electroencephalography has become the most widely used modality for signal acquisition in BCIs due to its high temporal resolution, noninvasiveness, relatively low cost, and high portability (RAMADAN; VASILAKOS, 2017).

The typical input patterns of BCIs are neurophysiological phenomena like Event-Related Synchronization/Desynchronization (ERS/ERD), Slow Cortical Potentials (SCP), P300 and Steady-State Visual Evoked Potentials (SSVEPs) (WOLPAW et al., 2002; HE et al., 2013). Among these patterns, SSVEP presents advantages for the development of a BCI, such as low portion of subjects unable to attain effective control (ALLISON et al., 2010; VOLOSYAK et al., 2011; GUGER et al., 2012), high signal-to-noise ratio (SNR) (BIN et al., 2009), and few or no training request (CHENG et al., 2002; BIN et al., 2009; VIALATTE et al., 2010; RAMADAN; VASILAKOS, 2017). In SSVEP-based BCIs, their command options can be codified into visual stimuli (Figure 1), in which each stimulus oscillates at a specified frequency (CHUMERIN et al., 2013).
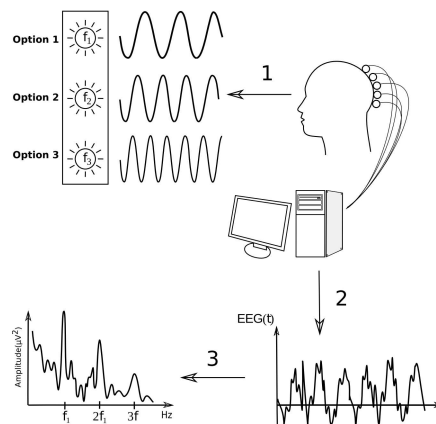
Figure 1 – Design and operation of a SSVEP-based BCI. 1) Subjects are asked to look at a flickering stimulus. 2) Brain signals are recorded during the stimulation. 3) the EEG signals are processed in order to extract representative features that are translated into commands. Adapted from (CHUMERIN et al., 2013).

Problem Statement

Users of conventional SSVEP-based BCIs are able to send commands to the computer by redirecting their gazing to the target stimulus location (Figure 1) (BASTOS-FILHO et al., 2014). However, paralyzed individuals who cannot control their muscular movements will have difficulties using these conventional SSVEP-based BCIs. In order to reduce the necessity of voluntary movements, some BCIs present two stimuli close to each other or superimposed, such as proposed by (KELLY et al., 2005; ALLISON et al., 2008; ZHANG et al., 2010; LESENFANTS et al., 2014; TELLO et al., 2016). However, stimuli proximity increases the neural competition in the visual cortex (FUCHS et al., 2008), implying a reduction of classification accuracy (NG; BRADLEY; CUNNINGTON, 2012; ZHANG et al., 2019). For that reason, Cotrina et al. (2017) proposed a SSVEP-based BCI composed of two stimuli presented together in the center of the subject's visual field, but in different longitudinal distance (called Depth-of-Field setup). This way, users were able to select one of both stimuli by adjusting their eye focus (COTRINA et al., 2017). Table 1 presents a summary of some characteristics of the aforementioned works.

However, as SSVEP response is often maximal on the visual cortex (NORCIA et al., 2015), all the aforementioned works acquired signals on the visual area. In fact, most of the existing SSVEP-based BCIs use electrodes located at occipital and parietal positions (ZHU et al., 2010). Nevertheless, a practical problem is that, generally this area is covered by hair, which causes complications in the electrode contacts with the skin (WANG et al., 2012; WEI et al., 2015; WANG et al., 2017). Moreover, BCI users with complete quadriplegia or in advanced stages of amyotrophic lateral sclerosis (ALS), generally have their head supported by a headrest (Figure 2), which makes it hard to acquire EEG signals from that area.
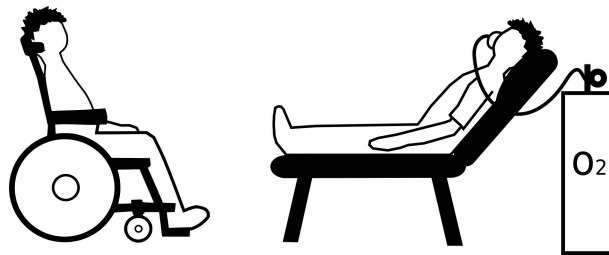
Figure 2 – Illustrations of daily routine of some patients with severe motor disabilities.

Measuring electroencephalogram (EEG) from hairless positions presents advantages to the user, and, recently, these kinds of BCI systems have been reported in the literature (WANG et al., 2012; NORTON et al., 2015; WANG et al., 2017). However, all these studies used stimuli in low and/or medium frequency bands, which prevent them to be practical BCI, as, in addition to producing visual fatigue, these frequency bands may increase the risk of photosensitive epileptic seizures and migraine headaches (ZHU et al., 2010).

Table 1 – Summary of the characteristics of related studies.

Study	Classes	Visual Stimulus	Stimulator Device	High-frequency	Hairless area
(KELLY et al., 2005)	2	Bilateral Squares with Letters	CRT monitor	No	No
(ALLISON et al., 2008)	2	Overlapped Lines	CRT monitor	No	No
(ZHANG et al., 2010)	2	Overlapped Dots	LCD monitor	No	No
(LESENFANTS et al., 2014)	2	Interlaced Squares	LED	No	No
(TELLO et al., 2016)	2	Rubin's Face-Vase	LED	No	No
(COTRINA et al., 2017)	2	Luminance	LED	No	No

Scientific Issue

A possible solution for the aforementioned problems reduction is the use of visual stimuli in high-frequency band ($\geq$ 30 Hz) (YIJUN et al., 2005; WON et al., 2015; CHABUDA; DURKA; ŻYGIEREWICZ, 2017) and measuring EEG at hairless areas. It is worth mentioning that studies applying below-the-hairline areas and high-frequency visual stimuli to implement a SSVEP-based BCI based on Depth-of-Field have not been addressed yet, despite this configuration being safe, practical and comfortable for people suffering from severe motor problems.

Objective

This thesis aims at developing a Brain-Computer Interface based on high-frequency SSVEP from below-the-hairline areas and Depth-of-Field.

Specific Objectives

- Evaluation of literature on the performance of methods for high-frequency SSVEPs detection.

- Analysis of the impact of reference electrode on SSVEP response from below-the-hairline areas.

- Evaluation of the influence of chromatic stimuli on SSVEP response from below-the-hairline and occipital areas.

- Study of the usage of eye focusing mechanism to modulate high-frequency SSVEP response from below-the-hairline.

- Development and evaluation of the proposed SSVEP-based BCI.

Contributions of this Thesis

New studies were conducted here in order to develop a reliable, accurate and practical BCI that can provide people with severe motor disabilities with an alternative communication way. The main contributions of this study include:

- Propose and demonstrate the feasibility of a novel BCI using high-frequency SSVEP from below-the-hairline areas.

- Investigate the impact of the reference electrode on SSVEP response from below-the-hairline areas.

- Investigate the relationship between SSVEP response and chromatic visual stimuli.

- Perform comprehensive analysis of signal processing methods for detection of high-frequency SSVEPs from occipital and below-the-hairline areas.

Structure of the Thesis

- Chapter 2 presents a brief introduction about the fundamentals of BCIs and SSVEP response.

- Chapter 3 presents the study about the influence of the reference electrode on SSVEP response obtained from hairless and occipital areas.

- Chapter 4 presents the study about the influence of chromatic stimuli on SSVEP obtained from hairless and occipital areas.

- Chapter 5 presents a comparison of methods for detection of high-frequency SSVEP.

- Chapter 6 presents the development and evaluation of the proposed high-frequency SSVEP-based BCI.

- Chapter 7 presents the conclusions of this study and future works.

2 Fundamentals

This chapter provides a brief introduction of the Brain, Vision and relevant concepts of Electroencephalography technique, Transient and Steady-State Visual Evoked Potentials and SSVEP-based BCIs.

2.1 Brain and Vision

2.1.1 Anatomy of Brain

The human brain is an important organ of the human body. The brain and the Spinal Cord form the Central Nervous System (CNS). Together with the Peripheral Nervous System, which connects the CNS to the limbs and organs, they form the Nervous System, which has fundamental importance in the control of the body functions. All the sensory information is received and processed by the Nervous System (GUYTON; HALL, 2006).

The brain is divided into two halves, the right and left cerebral hemispheres (Figure 3). They are connected to each other by the corpus callosum, a thick band consisting of an estimated 300 million neuronal axons that connect the two hemispheres. The two hemispheres communicate and cooperate with each other by means of constant information exchange through this neural connection (GUYTON; HALL, 2006).
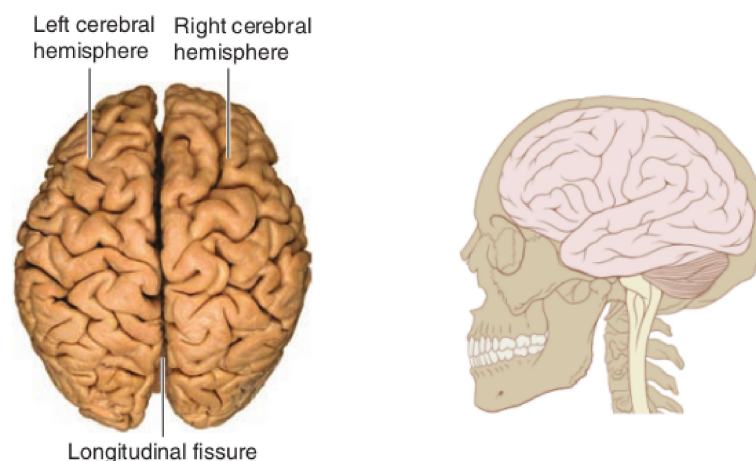
Figure 3 – Brain, superior and lateral view. Adapted from (SHERWOOD, 2015)

2.1.2 Cerebral Lobes

Distinct parts of the brain are specialized in different sensory and behavioral tasks, and all the information processing is done completely and in parallel. The first pictures of

the human brain during cognitive tasks were also snapped in the 1980s through use of positron emission tomography (PET) scans (Figure 4).
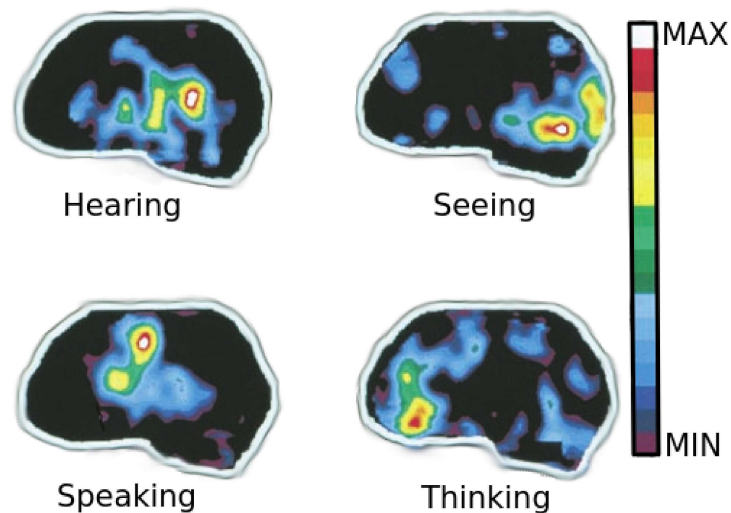
Figure 4 – PET scans of cerebral cortex during different tasks. Adapted from (SHER-WOOD, 2015)

As depicted in Figure 5, the cerebral cortex can be divided into four main areas (lobes): the frontal, temporal, parietal and occipital lobes (GUYTON; HALL, 2006; KANDEL et al., 2013).
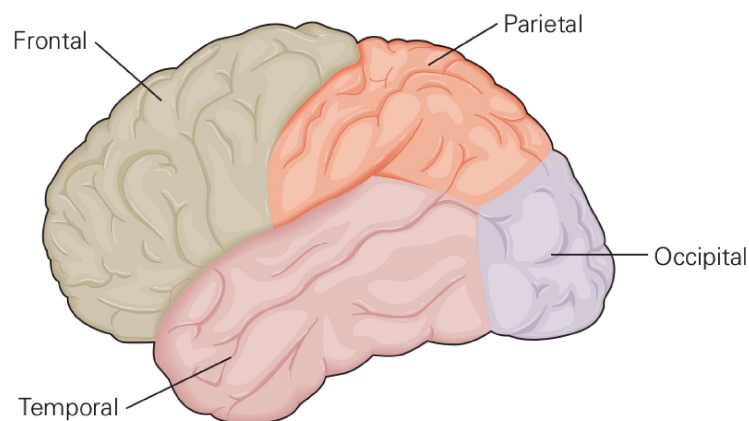
Figure 5 – Distribution of the cerebral cortex. Adapted from (KANDEL et al., 2013)

The temporal lobe receives and processes auditory information and this area is related to the identification and naming of objects. The frontal lobe, which includes the motor cortex and pre-motor cortex and the prefrontal cortex, is involved in action and movement planning, as well as abstract thinking. The parietal lobe is the primary somatosensory cortex and receives information on touch and pressure. The occipital lobe receives and processes visual information.

2.1.3 Eye

The eye is a complex optic system that contains about 125 million photoreceptors specialized in turning light into electrical signals (GUYTON; HALL, 2006). A schematic diagram of a horizontal, sectional view through a human eye is shown in Figure 6.
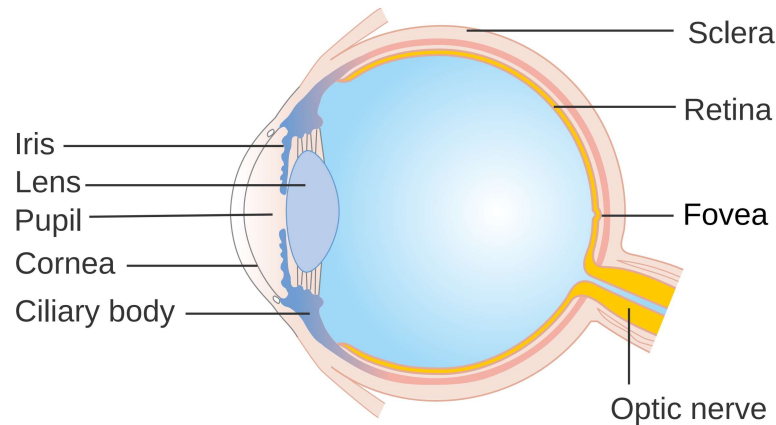
Figure 6 – Schematic diagram of the human eye. Adapted from (KANDEL et al., 2013)

The cornea and the sclera are the transparent membrane over the front of the eye and the white membrane around the sides and back of the eyeball, respectively. The iris, which is the colored part of the eye, controls the aperture of the pupil regulating the amount of light entering the eye. The pupil is the aperture at the center of the iris, through which light enters the eye. The crystalline lens of the eye or lens is a transparent and flexible structure; by changing its curvature through the contraction or relaxation of the intrinsic muscles of the eye, light coming from different sources is projected on the back of the eye (GUYTON; HALL, 2006; KANDEL et al., 2013).

2.1.4 Photoreceptors

The photoreceptors are cells that transform the light energy into electrical signals to CNS (SHERWOOD, 2015). Rods and cones are two types of photoreceptors in human eyes. The fovea is eye region where the cones are concentrated. These receptors have high acuity in bright light that makes the fovea essential for daytime vision. Rods are designed to provide some vision in dim light. Figure 7 illustrates the relative distribution of the cones and rods on the retina.

Three types of cones are in found human eyes (Figure 8). The first one responds by the light of long wavelengths, arriving at a red color; this type is sometimes called L (Long). The second type responds to the light of medium wavelength, reaching a maximum of a green color, and is abbreviated M (Medium), to medium. The third type responds more to the short wavelength of light, of a bluish color, and is designated S (Short). The three types have peak wavelengths near 564-580 nanometers (nm), 534-545 nm and 420-440 nm,
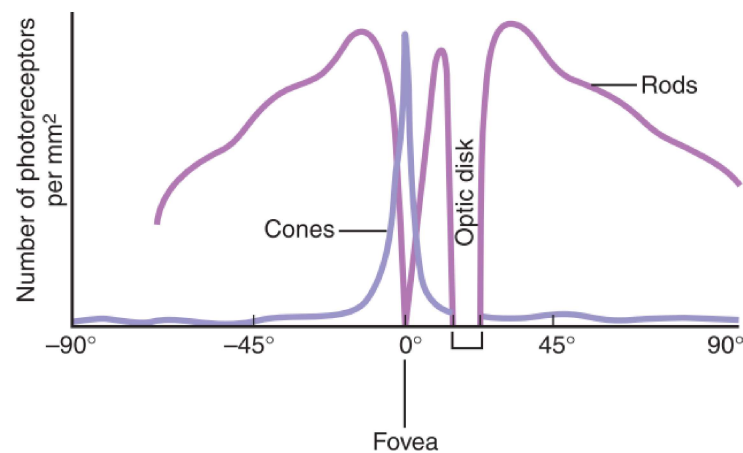
Figure 7 – Relative distribution of the cones and rods on the retina. Adapted from (KAN-
DEL et al., 2013)

respectively. The difference between the signals received from the three cone types allows
the brain to perceive all possible colors making color vision possible (SHERWOOD, 2015).
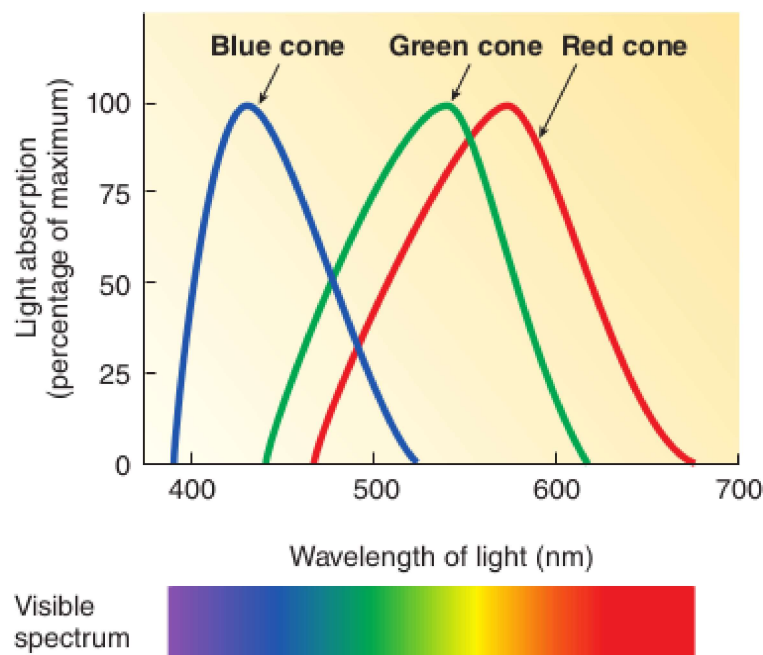
Figure 8 – Sensitivity of the three types of cones to different wavelengths. Adapted from
(SHERWOOD, 2015)

2.1.5   Visual Pathways

The visual pathway describes the anatomical pathway by which electrical signals
generated by the retina are sent to the brain (KANDEL et al., 2013). The visual pathway
includes the retina, optic nerve, the Lateral Geniculate Nucleus (LGN) and the visual
cortex (Figure 9).
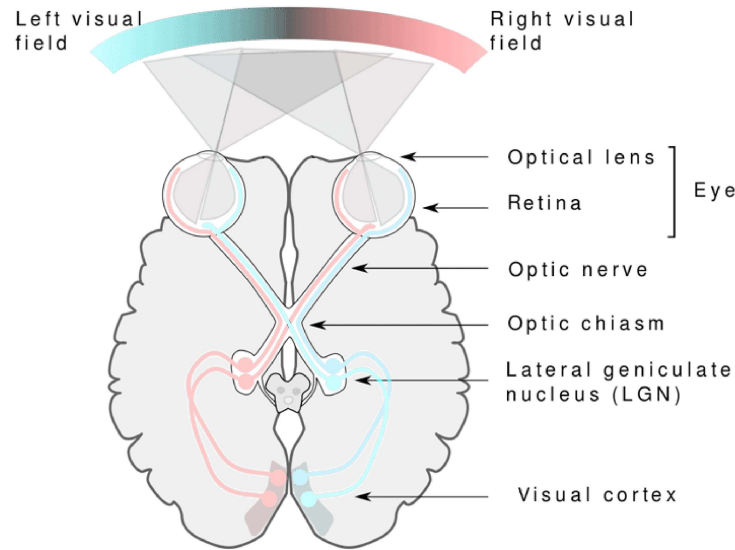
Figure 9 – Functional representation of visual pathways. Adapted from (KANDEL et al., 2013)

The visual cortex in the right cerebral hemisphere receives its input from the left half of the visual field, and the visual cortex in the left hemisphere receives its input from the right half of the visual field (KANDEL et al., 2013; GUYTON; HALL, 2006)

2.1.6   Eyes Focusing Mechanism

The mechanism to adjust the focus of the eye that change the shape of the lens is called accommodation (SHERWOOD, 2015). Depending on the distance of the object, ciliary muscles attached to the lens, contract or relax, changing its curvature. Thus, a sharp retinal image is produced. This mechanism for a near target occurs when the lens of the eyes forms a more spherical shape to bring the object into the focus. On the other hand, lens is elongated for focusing distant objects (Figure 10). Depth-of-field is the range of distances near the point of focus where the eye imaged an object as sharp. Objects out of the point of focus produce blurred appearance (PENTLAND, 1987).

Far source   Near source
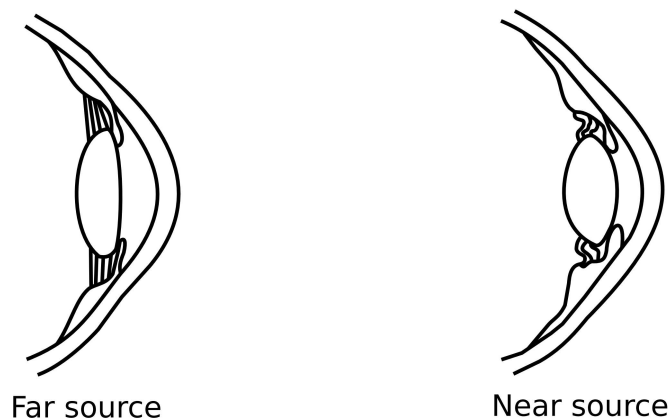
Figure 10 – Mechanism of accommodation of the eyes. Adapted from (SHERWOOD, 2015).

2.2 Electroencephalography

Electroencephalography is an electrophysiological monitoring method to record electrical activity of the brain. The EEG signals consist of the summed electrical activities of populations of neurons (Figure 11). The neurons are excitable cells with electrical properties, and their activity produces electrical and magnetic fields that may be recorded by means of electrodes at the scalp (MULERT; LEMIEUX, 2009).
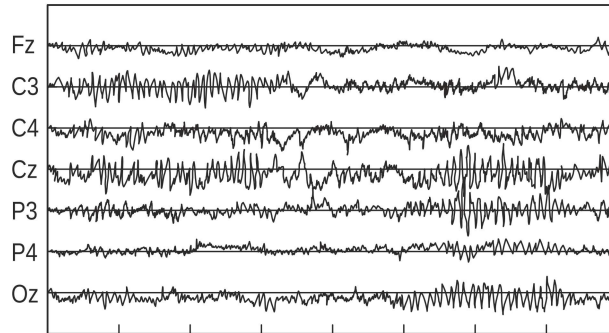
Figure 11 – Example of EEG signals of a group of channels.

The EEG recording system consists of electrodes, amplifiers, A/D converter, and a recording device. The electrodes acquire the signal from the scalp, and the amplifiers process the analog signal to enlarge the amplitude of the EEG signals so that the A/D converter can digitize the signal more accurately. Finally, the recording device, which may be a personal computer or similar, stores, and displays the data. The amplitude of this electrical biosignal is in the order of microvolts (NICOLAS-ALONSO; GOMEZ-GIL, 2012; PUCE; HÄMÄLÄINEN, 2017).

The EEG signal is typically measured as the potential difference over time between signal or active electrode and reference electrode. An extra third electrode, known as the ground electrode is used to measure the differential voltage between the active and the reference electrodes. The minimal configuration for EEG measurement therefore consists of one active, one reference and one ground electrode. Furthermore, electroencephalography presents features like high temporal resolution, relative low cost, high portability, and few risks to the users (NICOLAS-ALONSO; GOMEZ-GIL, 2012).

2.2.1 Standard System of Electrode Placement

The 10/20 system or International 10/20 system is an internationally recognized method to describe the location of scalp electrodes. The system is based on the relationship between the location of an electrode and the underlying area of the cerebral cortex. The electrode locations are determined by dividing the perimeter into 10% and 20% intervals. An extension to the 10/20 system is the 10/10 system, which is characterized by intervals

of 10%, providing a higher channel density (JURCAK; TSUZUKI; DAN, 2007). Figure 12 shows electrode positions according to the American Electroencephalographic Society.
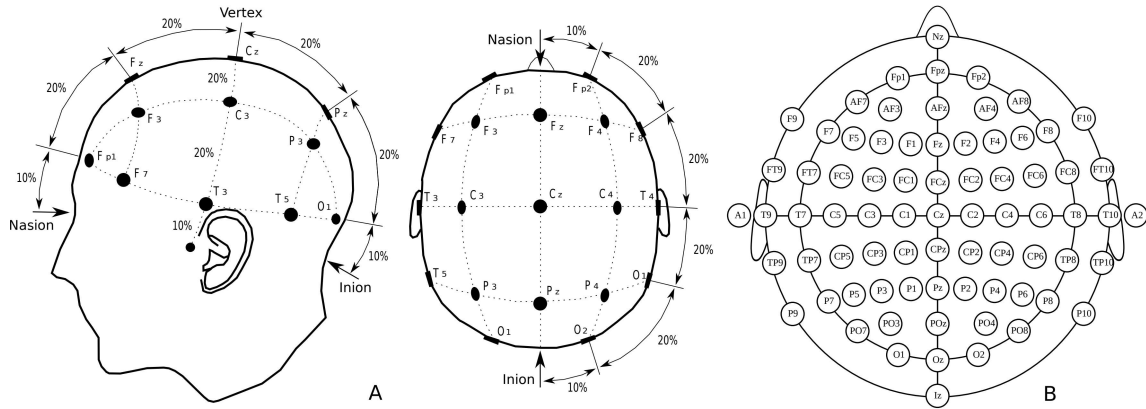
Figure 12 – Location and nomenclature of the 10-20 and 10-10 system. The electrodes are named by a capital letter corresponding to the initial of the brain lobe where they are placed (*F*, *C*, *P*, *O* and *T* for Frontal, Central, Parietal, Occipital and Temporal, respectively), followed by an even number for the right hemisphere and an odd number for the left hemisphere. The letter *A* is used for electrodes placed in the ear. For the electrodes placed in the frontal lobe, near the nasion, the letter *p* is added (Fp = Frontal pole). For the electrodes in the line connecting the nasion to the inion, the letter *z* is added. Adapted from (GRAIMANN; ALLISON; PFURTSCHELLER, 2010a)

2.3   Transient and Steady-State Visual Evoked Potential

2.3.1   Transient Visual Evoked Potential

An evoked potential is the electrical response recorded from the human nervous system following presentation of a stimulus. This response can be measured by an EEG device (ODOM et al., 2004). Transient Visual Evoked Potentials (TVEP) refer to electrical potentials initiated by brief visual stimuli, which are recorded from the scalp traditionally overlying the visual cortex. These responses occur when a subject observes a visual stimulus, such as a flash of light or a pattern on a monitor. TVEP are used primarily to measure the functional integrity of the visual pathways from the retina via the optic nerves to the visual cortex of the brain. Their waveforms are usually extracted from the EEG signals by averaging. Such as shown in Figure 13, TVEP waveforms are represented using amplitude and time (latency) measurements (ODOM et al., 2004).

TVEP are obtained when the stimulus rate is low and the response is recorded over one single stimulus cycle. A typical TVEP waveform consists of N75, P100 and N135 peaks which are shown at about 75, 100, and 135 milliseconds after visual stimulation, respectively. Any abnormality that affects the visual pathways or visual cortex in the brain can affect the TVEP waveform.
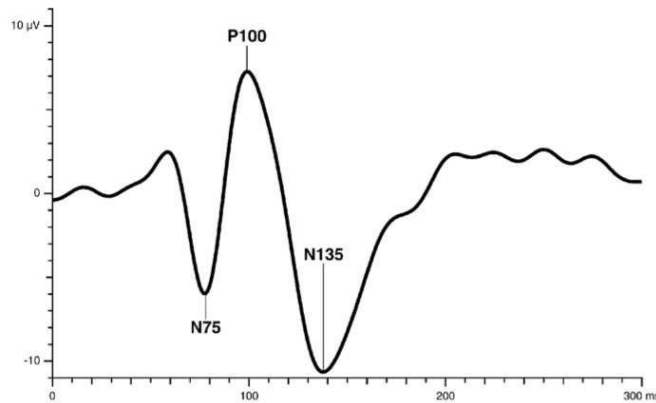
Figure 13 – A normal pattern TVEP measured in EEG. Adapted from (ODOM et al., 2004).

2.3.2 Steady-State Visual Evoked Potential

Steady-State Visual Evoked Potential (SSVEP) is the elicited response in the visual cortex by light stimuli flickering at a constant frequency (ZHU et al., 2010). These potentials manifest as an oscillatory component in the EEG signal with the same frequency (and/or its harmonics) of the visual stimulation (ZHU et al., 2010). SSVEP can normally be evoked up to 90 Hz (HERRMANN, 2001), and three stimuli bands can be identified: low (up to 12 Hz), medium (12–30 Hz), and high-frequency ($\geq$30 Hz) (REGAN, 1989; ZHU et al., 2010; RAMOS et al., 2011).

The steady-state potentials are distinguished from transient potentials by their constituent discrete frequency components which remain relatively constant in amplitude and phase over a long time period (REGAN, 1989; VIALATTE et al., 2010). Consequently, the amplitude distribution of the spectral content of SSVEP, with characteristic SSVEP peaks, remains stable over time (Figure 14). Because these characteristics are constant, many applications can be derived from SSVEP properties.

2.3.3 SSVEP-based BCIs

Such as aforementioned, Brain-Computer Interfaces (BCIs) are systems that allow the control of external devices using measured signals of brain activity (WOLPAW et al., 2002). Because BCIs do not use neuromuscular commands as input, the advent of these interfaces allows us to establish an alternative pathway of interaction with the world for people with severe motor impairment (WOLPAW et al., 2002; GRAIMANN; ALLISON; PFURTSCHELLER, 2010b).

On the other hand, SSVEP-based BCIs have attracted the interest of many researchers in recent years due to outstanding accuracy, low portion of subjects unable to attain effective control (ALLISON et al., 2010; VOLOSYAK et al., 2011; GUGER et al.,
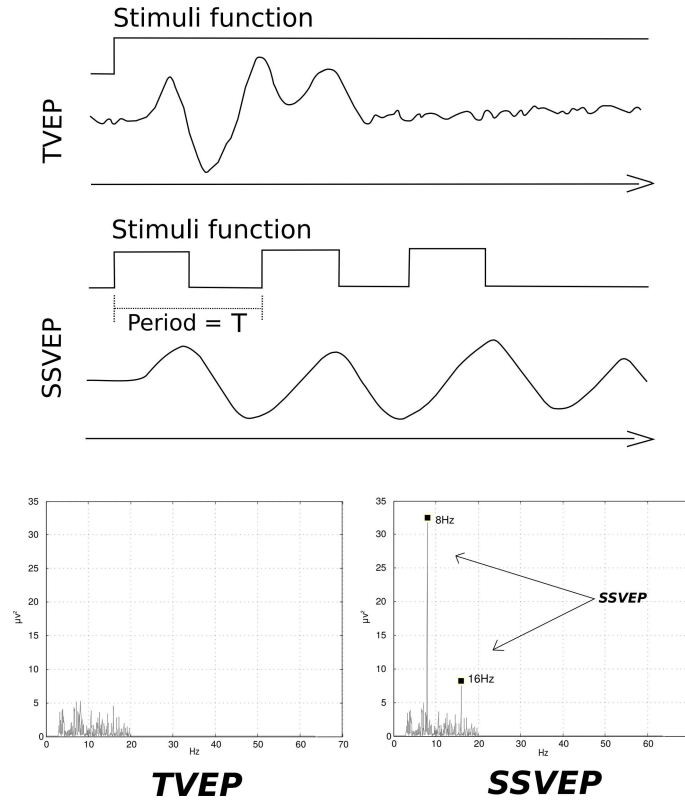
Figure 14 – Example of a TVEP and SSVEP response in time domain and frequency domain. Adapted from (VIALATTE et al., 2010)

2012), higher information transfer rate (ITR) (BIN et al., 2009) and few or no training requirement (CHENG et al., 2002; BIN et al., 2009; VIALATTE et al., 2010; RAMADAN; VASILAKOS, 2017).

The system commands can be codified into visual stimuli with specified frequency of oscillation (CHUMERIN et al., 2013). Thus, when a subject gazes at one of the stimulus, an SSVEP is evoked in their brain (VIALATTE et al., 2010; NORCIA et al., 2015), which can be detected in the EEG signal. These measurements can then be used as control commands to the BCI with precision (ALLISON et al., 2010). Figure 15 presents a diagram of an SSVEP-based BCI.

Three types of stimuli have mainly been used so far for BCIs (Figure 16): light stimuli (blinking Light-Emitting Diodes-LEDs), simple graphics such as flickering squares on an LCD computer screen and complex graphics flickers (e.g., alternatively reversing checkerboards) (ZHU et al., 2010).

The traditional metrics for BCI evaluation are classification accuracy and Information Transfer Rate (ITR) (VIALATTE et al., 2010):

- Accuracy is the percentage of correctly classified commands.

- ITR is a standard measure of the amount of information transferred per unit of time,
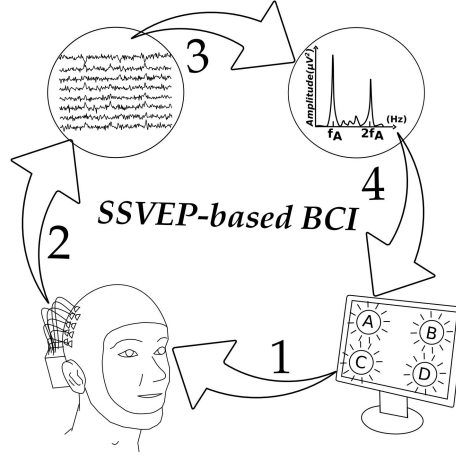
Figure 15 – Diagram of the SSVEP-based BCI. (1) Subject gazes at Target A flickering at frequency f_A. (2) EEG signals are measured from the scalp and recorded on a computer. (3) The data is processed, and features such as peaks at f_A and its harmonics are extracted. (4) The features are classified and translated into commands to the application.
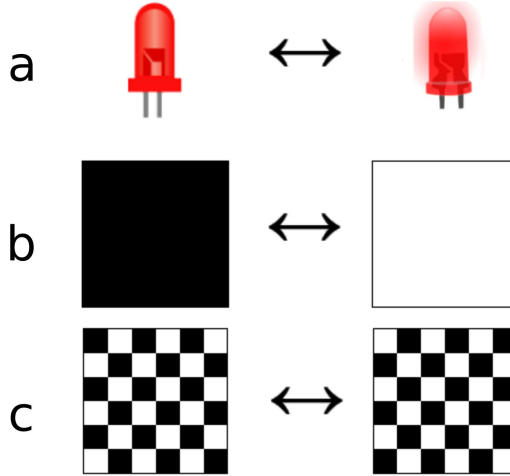
Figure 16 – Types of Visual Stimulation: a) Light stimuli. b) Simple graphics stimuli. c) Complex graphics stimuli.

which is defined by Equation 2.1:

$$ITR = s \left[log_2(N) + plog_2(p) + (1-p)log_2 \left(\frac{1-p}{N-1} \right) \right], \qquad (2.1)$$

where N is number of commands, p is accuracy value and s commands performed per minute.

2.3.4 Applications

Nowadays, due to its robustness and few or no calibration demand for BCI usage, SSVEP responses are being widely applied in BCIs to develop assistive technology (AT), with different categories (Figure 17), according to their applications:

- Computer Interaction and Alternative Communication: (NAKANISHI et al., 2014; WU et al., 2011; CHEN et al., 2015b; HWANG et al., 2012; VOLOSYAK et al., 2009; DIEZ et al., 2011; WON et al., 2015; CHABUDA; DURKA; ŻYGIEREWICZ, 2017; YIN et al., 2014)

- Mobility: (KWAK; MÜLLER; LEE, 2015; XU et al., 2012; MÜLLER; BASTOS; SARCINELLI, 2013; DIEZ et al., 2013; CAO et al., 2014)

- Entertainment: (LALOR et al., 2005; CHUMERIN et al., 2013; SHYU et al., 2010; MARTIŠIUS; DAMAŠEVIČIUS, 2016; LEGENY; VICIANA-ABAD; LECUYER, 2013; AKHTAR et al., 2014; CHEN et al., 2017)

- Neural Prosthetics and Rehabilitation Systems: (MULLER-PUTZ; PFURTSCHELLER, 2008; ZHAO et al., 2016; PFURTSCHELLER et al., 2010; ORTNER et al., 2011; SAKURADA et al., 2013; ZENG et al., 2017; XIE; MENG, 2017; SAVIĆ; KISIĆ; POPOVIĆ, 2011)

- Ambient Assisted Living: (GAO et al., 2018; TELLO et al., 2015; PUNSAWAD; WONGSAWAT, 2012; MORA; MUNARI; CIAMPOLINI, 2016)
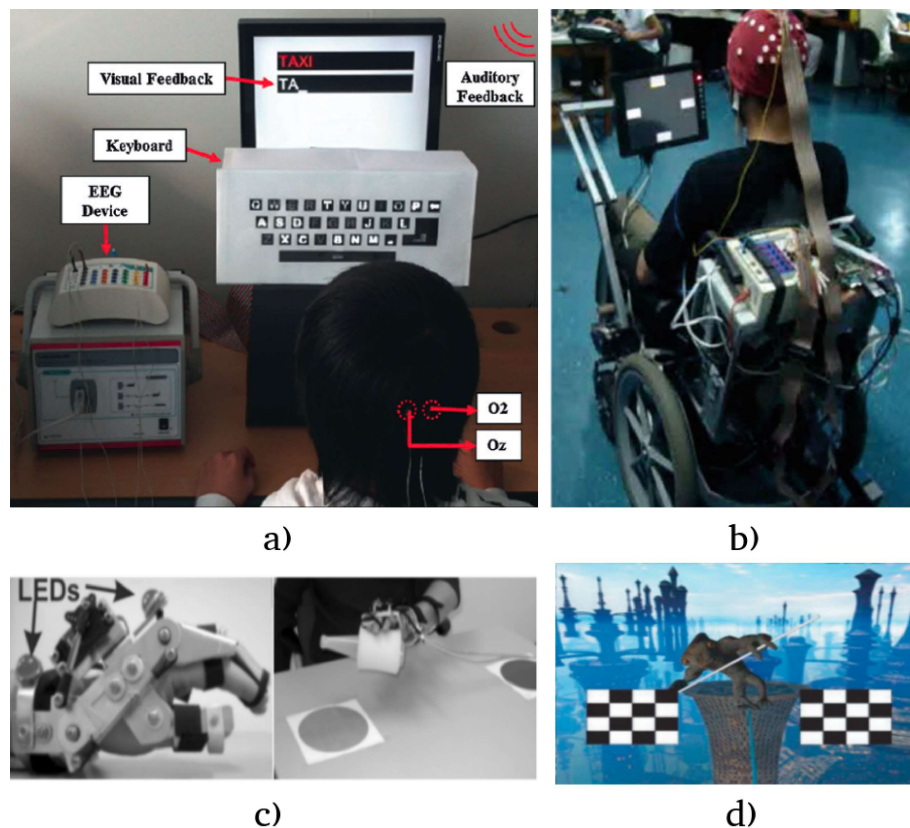
Figure 17 – Examples of assistive applications using SSVEP response: a) Alternative Comunication (HWANG et al., 2012); b) Mobility (MÜLLER; BASTOS; SARCINELLI, 2013); c) Neural Prosthetics (ORTNER et al., 2011); d) Entertainment (LALOR et al., 2005).

3 A study of SSVEP from below-the-hairline areas

This chapter presents the evaluation of the montage of channels to measure SSVEP from below-the-hairline areas when a subject is stimulated at low-, medium- and high-frequency ranges. Twelve healthy subjects participated in this study. The elicited SSVEP was evaluated in terms of amplitude and signal-to-noise ratio (SNR).

3.1 Introduction

Recent studies have proposed different approaches to Brain-Computer Interfaces (BCI) based on Steady-State Visual Evoked Potentials (SSVEP). These approaches employ EEG signals collected from easily accessible below-the-hairline areas[1]. For example, Norton et al. (2015) detected SSVEPs with an electrode positioned behind-the-ear. Hsu et al. (HSU et al., 2016) presented a binary SSVEP-based BCI system using an EEG electrode montage placed on the frontal and temporal regions (Fpz-TP9) and employing medium-frequency stimuli. Wang et al. (2017) detected SSVEP from behind-the-ears with the reference electrode at the frontal region, at low- and medium-frequency range.

The reference electrode position and the stimulation frequency affect the SSVEP measured on the scalp (occipital area) (VIALATTE et al., 2010). However, the influence of these factors on SSVEP from below-the-hairline areas in the three frequency bands was not addressed. Thus, this study aims to investigate how reference electrode and the frequency bands (low, medium and high bands) affect the SSVEP measured on hairless areas. The objective of this study is to perform a comparison about SSVEP obtained from hairless regions. The SSVEP is evaluated in terms of amplitude and SNR.

3.2 Materials and Methods

3.2.1 Participants

Twelve healthy subjects (ages 26.1 ± 4.1; 6 F and 6 M) with normal or corrected to normal vision participated in this study. The EEG recordings were conducted in a laboratory with low background noise and dim luminance. The study was approved by the Ethics Committee from the School of Exact, Physical and Natural Sciences from the

---

[1] In studies related to the study of epileptic seizures, the use of below-the-hairline positions (frontal, behind-the-ears) has then already been employed (BRIDGERS; EBERSOLE, 1988; YOUNG et al., 2009; BUBRICK; BROMFIELD; DWORETZKY, 2010)

National University of San Juan Argentina (act #7). Prior to participating in this study, all volunteers read an information sheet and signed a consent form. The subjects did not receive any financial compensation for their participation.

3.2.2   Data acquisition

The EEG signals were acquired with a Grass 15LT amplifier system, and digitized with a NI-DAQ-Pad6015. The sampling frequency was set at 256 Hz for each channel. The cut-off frequencies of the analog pass-band filter were set to 1 and 100 Hz. Additionally, a notch filter for 50 Hz was applied to remove powerline interference.

To evaluate how the electrode montage affects the measurement of SSVEP, thirteen channel configurations were evaluated, as shown in Table 2. The ground electrode (GND) was placed at A2 (Figure 18).
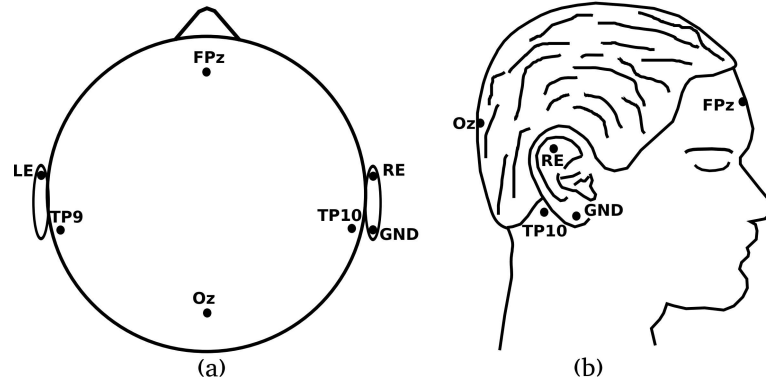
Figure 18 – Positions on the scalp where the electrodes were located: (a) top view and (b) side view.

Table 2 – EEG analyzed channels.

Groups	Occipital	Frontal	Temporal	Temporal-Frontal
	Oz-Fpz	Fpz-LE	TP9-LE	TP9-Fpz
	Oz-TP9	Fpz-RE	TP9-RE	TP10-Fpz
Channels	Oz-TP10		TP10-LE	
	Oz-LE		TP10-RE	
	Oz-RE			

3.2.3   Visual Stimulation and Acquisition Protocol

The visual stimulus was composed of a light-emitting diode (LED) that illuminates a diffusion board of 4cm x 4cm. For this thesis, we analyzed the range of frequencies from 5 to 45 Hz (with steps of 5 Hz). The frequency of the LED was precisely controlled with an FPGA Xilinx Spartan3E on a Nexys board (Digilent Inc.). Therefore, the stimuli range covers the three SSVEP bands (low-, medium- and high-frequency).

Each subject sat in a chair at 60 cm from the stimulus. The experiment consisted of five runs and each run was composed of trials, one per each stimulation frequency. The stimulation frequencies were presented in random order to each volunteer. Each trial lasted 7 s, with a varying separation between trials from 2 s up to 4 s, to avoid expectation effect. The trial begins with a beep (at t = 0 s) and 2 s later the stimulus is turned on. The stimulus stays on until the end of the trial at t = 7 s. At this moment, a feedback is presented to the volunteer, indicating whether the SSVEP was detected or not. The volunteer could relax for 2-5 min before beginning the next run.

3.2.4   EEG Data Analyzing

First, the EEG was digitally filtered with a band-pass Butterworth filter, order 6, bandwidth 3-70Hz. An EEG segment of 5 s was extracted from t = 2 s and t = 7 s, and the magnitude of the frequency components of the signal was calculated based on the Discrete Fourier Transform (DFT) of the signal (ARFKEN; WEBER, 1999).

The SNR of the SSVEP at a single channel is defined as the ratio of signal magnitude of the frequency f to the mean amplitude of the K neighboring frequencies (WANG et al., 2006; WANG et al., 2017):

$$SNR = \frac{K \times F(f)}{\sum_{n=1}^{K/2}[F(f + n\Delta f) + F(f - n\Delta f)]},$$
(3.1)

where $F(f)$ is the magnitude of signal of the frequency f, Δf is the frequency resolution (0.2 Hz in this study), and K was set to 8 (i.e., four frequencies on each side) (CHEN et al., 2014).

The one-way analysis of variance (ANOVA) was applied to the data. The statistical tests were run for each stimulation frequency, and then we analyzed the behavior of the SSVEP from every channel in each frequency. Following, the Tamhane T2 was used for post hoc tests.

3.3   Results and Discussion

It is important to point out that the notch filter at 50Hz may affect the SSVEP at 45 Hz and, thus, they presented lower amplitudes. Moreover, the SSVEP measured at 5 Hz may be diminished by the high-pass filter response.

Figure 19 and 20 show the amplitude and SNR of the SSVEPs from all evaluated channels.

Considering the occipital region, many studies were performed analyzing variations of SSVEP amplitude in relation to stimulation frequencies. Pastor et al. showed that the
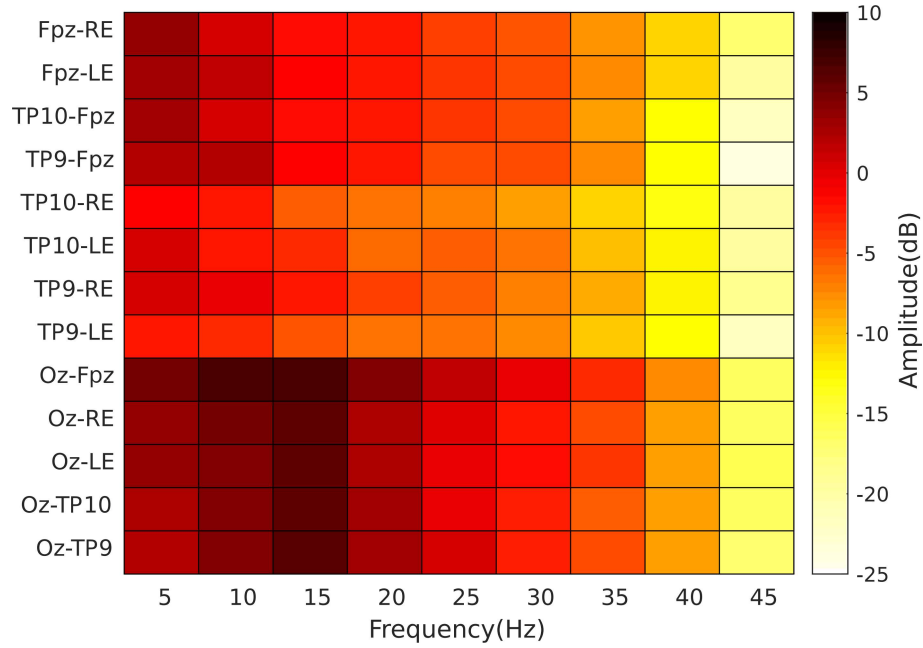
Figure 19 – Amplitude of the SSVEPs from all evaluated channels.
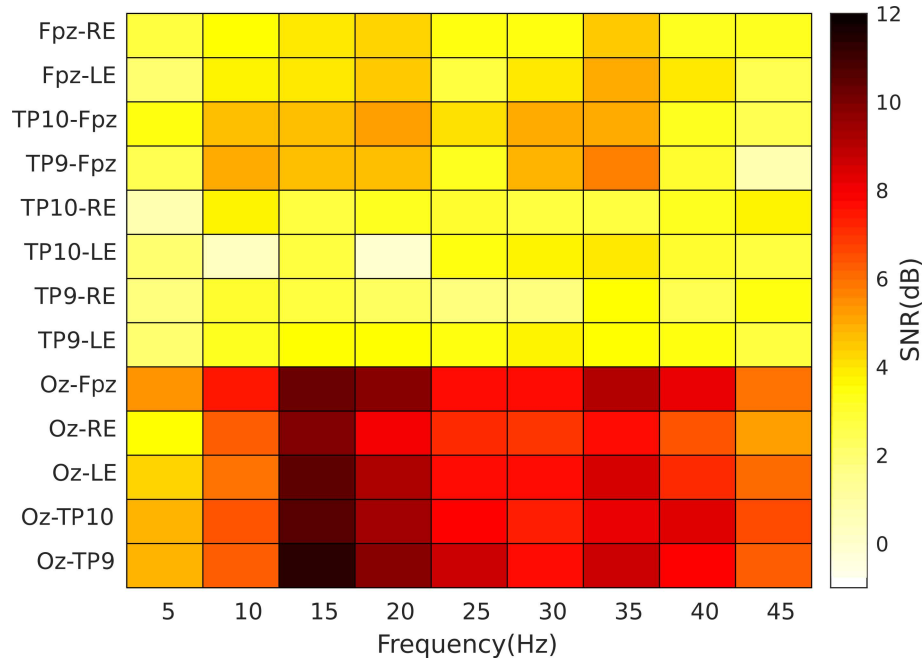
Figure 20 – SNR of the SSVEPs from all evaluated channels.

largest amplitude of response at the occipital area occurs at 15 Hz (PASTOR et al., 2003). Wang et al. reported that SSVEP amplitudes exhibit three maxima centered on 15, 31 and 41 Hz (WANG et al., 2006). Jukiewicz et al (JUKIEWICZ; CYSEWSKA-SOBUSIAK, 2016) found that human brain response is the strongest when presented with stimuli flashing with frequency of about 16 Hz.

In our research, the SSVEP on Oz electrode was acquired for comparison purposes. The occipital group achieved higher SSVEP amplitudes than other groups, as expected.

Furthermore, occipital group presented higher SNR, particularly up to 40 Hz (with *p*-value < 0.05 for most frequencies). In agreement with the research previously mentioned, we found stronger SSVEP around 15 Hz (Figure 20).

For hairless positions, the temporal group presented lower amplitude values than occipital, frontal and temporal-frontal configurations. Among the temporal group, TP9-RE channel showed higher SSVEP amplitudes than other channels between 5 Hz and 20 Hz (Figure 19). TP10-LE channel is the second best channel (after TP9-RE) in the same frequency range (5-20 Hz). Additionally, both channels showed similar values for other stimulation frequencies. The highest SNR for the SSVEP on hairless areas was found in the measurements obtained by TP9-Fpz and TP10-Fpz (Figure 20).

In summary, it was found that occipital positions present the best SNR. On the other hand, the best channel to measure SSVEP from the non-hair positions (up to 40 Hz) are temporal-frontal positions (TP9-FPz and TP10-FPz). Our findings suggest that the SNR of SSVEP can be improved using the temporal-frontal montage.

4 Evaluating of Chromatic and Luminance Stimuli

This chapter presents a study of chromatic and luminance stimuli in low-, medium-, and high-frequency stimulation to evoke steady-state visual evoked potential (SSVEP) in below-the-hairline areas. Twelve healthy subjects participated in this study. The electroencephalogram (EEG) was measured on occipital (Oz) and left and right temporal (TP9 and TP10) areas. The SSVEP was evaluated in terms of amplitude and signal-to-noise ratio (SNR).

4.1 Introduction

Recent SSVEP-based BCI studies have employed EEG signals measured from below-the-hairline areas (frontal and behind-the-ears areas) (NORTON et al., 2015; WANG et al., 2017; HSU et al., 2016). However, these works used stimuli based only on luminance modulation (on/off stimulus). On the other hand, visual stimuli that use colors (green-blue or green-red) and luminance combination can increase the evoked response (TAKANO et al., 2009; IKEGAMI et al., 2012; AMINAKA; MAKINO; RUTKOWSKI, 2014; SAKURADA et al., 2015; CHEN et al., 2017). Moreover, it was found that color information is mediated by specialized neurons that are clustered within the temporal areas (CONWAY; MOELLER; TSAO, 2007). Besides, there are color-selective neurons in the inferotemporal cortex (KOIDA; KOMATSU, 2007). The inferotemporal cortex receives projections from the primary visual cortex (ventral pathways) (MISHKIN; UNGERLEIDER, 1982; GOODALE; MILNER, 1992), which are both color-sense-associated and object recognition pathways that detect colors.

Therefore, in this chapter, we present a comparative study of chromatic and luminance stimuli flickering at low-, medium-, and high-frequencies to evoke SSVEP responses in behind-the-ears areas. Basically, this study aims to answer three questions: (1) What is the influence of chromatic and luminance stimuli on SSVEP from behind-the-ears? (2) What is the best combination (green-blue or green-red[1])? (3) How is the SSVEP response evoked by these stimuli in low-, medium-, and high-frequency bands? Therefore, the results of the current work will help in the development of more accurate and comfortable BCI systems.

---

[1] We did not use the blue-red combination, as these colors are the worst case for photosensitive epilepsy, especially at 15 Hz (PARRA et al., 2007)

4.2   Materials and Methods

4.2.1   Data Acquisition

Twelve healthy subjects (ages 26.1 ± 4.1; 6 F and 6 M) with normal or corrected-to-normal vision participated in this study. The EEG recordings were conducted in a laboratory with low background noise and dim luminance. Previous to participation in this study, all volunteers read an information sheet and provided written consent to participate. Ethical approval was granted by the institutional ethics committee. The subjects did not receive any financial reward for their participation.

The EEG was measured over occipital (Oz) and left and right temporal (TP9 and TP10) areas (Figure 21). The ground electrode was placed at A2. The EEG signals were acquired with a Grass 15LT amplifier system, and digitalized with a NI-DAQ-Pad6015 (sampling frequency: 256 Hz). The cut-off frequencies of the analogical pass-band filter were set to 1 and 100 Hz. Additionally, a notch filter for 50 Hz line interference was applied.

(a)   (b)
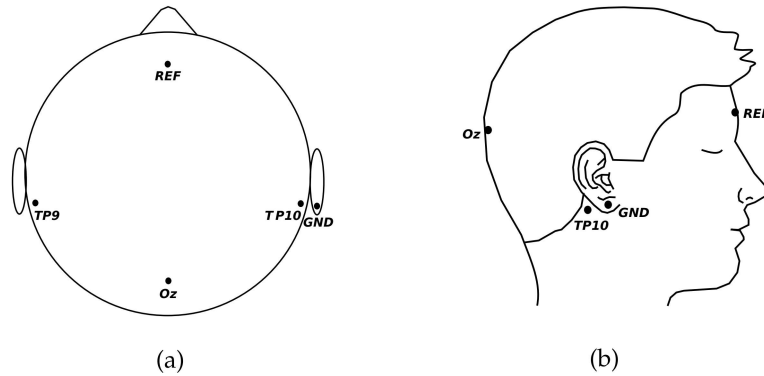
Figure 21 – Positions on the scalp where the electrodes were located. (**a**) Top view of positions; (**b**) Side view of the positions. Oz: occipital area; TP9: left temporal area; TP10: right temporal area; REF: reference electrode; GND: ground electrode.

4.2.2   Visual Stimulation

The visual stimulation was performed by light-emitting diodes (LEDs) that illuminated a diffusion board of 4 cm × 4 cm. The LEDs were red, blue, green, and white. Each LED could flicker at different frequencies from 5 Hz to 65 Hz with an interval of 5 Hz. Therefore, the stimulation range comprised the three SSVEP bands (low-, medium-, and high-frequency). The frequency of the LEDs was precisely controlled with an Xilinx Spartan3E field-programmable gate array (FPGA) on a Nexys board (Digilent Inc., Pullman, USA). The 50 Hz frequency was not used as a stimulation frequency, because this is the Argentinian power line frequency.

The setup consisted of three different stimuli (Figure 22). The first stimulus was white (W) LED for the luminance condition. The other two stimuli were green-red (G-R) stimulus and green-blue (G-B) stimulus. Figure 22 shows the transition of the two states of the visual stimuli. Each state remained activated for half of the period of the stimulation frequency (f = 1/T, where T is the period). For the luminance stimulus (W), the two states represented the light on and off. For the G-R and G-B stimulus, the two states were green-red and green-blue, respectively.
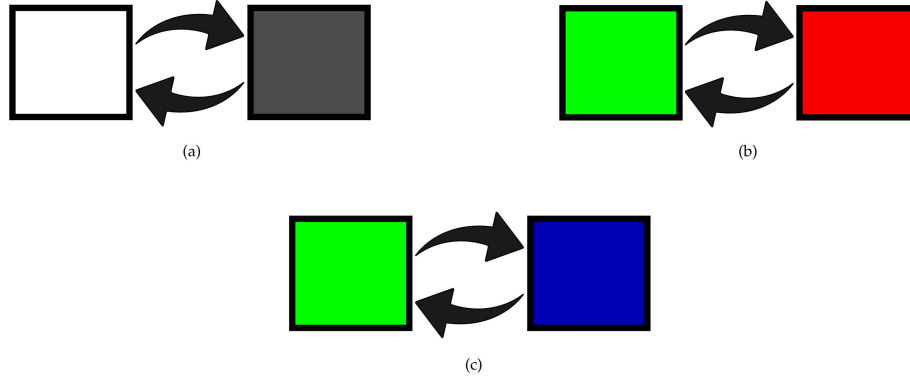
Figure 22 – Visual stimulation used for the experiments: (**a**) Luminance stimulus (white, W); (**b**) green-red (G-R) stimulus; (**c**) green-blue (G-B) stimulus.

4.2.3   Experimental Protocol

Each subject sat in a chair at 60 cm from the stimulus. The experiment was divided into five runs (Figure 23a). At each run, the three possible stimuli (G-R, G-B, and W) were showed to the volunteer (Figure 23b). At each colored stimulus, the 12 frequencies were presented. Thus, each stimulus comprised 12 trials, and each trial lasted 7 s (Figure 23c). Thus, 12 trials (one per frequency) of the same colored stimulus were presented to the volunteer. Later, the process was repeated for the other two colored stimuli, which comprised a run. Finally, the run was repeated five times. The stimulation frequencies and the colored stimuli were randomly presented to each volunteer. In order to avoid expectation effects, a variable separation time (2–4 s) between trials was used. The trial began with a beep (at t = 0 s), and 2 s later the stimulus was turned on. The stimulus stayed on until the end of the trial at t = 7 s. At this moment, a feedback was presented to the volunteer indicating whether the SSVEP was detected or not. The volunteer could relax for 2–5 min.

4.2.4   EEG Signal Processing

The EEG was preprocessed using a Butterworth filter, order 6, with cut-off frequencies set at 3 and 70 Hz. Later, the EEG between t = 2 s and t = 7 s was extracted for analyzing in the next step. Then, the magnitude of the frequency components of the
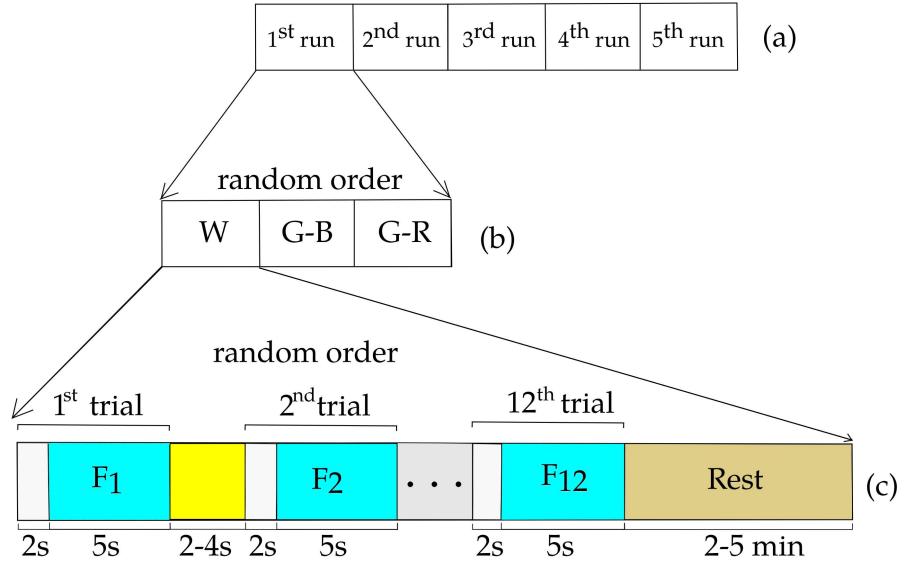
Figure 23 – Protocol of the experiment: (**a**) experiment divided into five runs; (**b**) three colored stimuli presented in random order to each volunteer; (**c**) 12 frequencies randomly presented for each colored stimulus.

signal was calculated based on the Discrete Fourier Transform (DFT) of the signal. The signal-to-noise ratio (SNR) measurement was computed based on Equation 3.1.

4.2.5   Statistical Evaluation

For the statistical analysis of the results, the Friedman test for simultaneous comparison of more than two groups was used. Post-hoc pairwise comparisons using Wilcoxon signed-rank test were also conducted, in which a level of $p < 0.05$ was selected as the threshold for statistical significance.

4.3   Results

4.3.1   Amplitude

Figure 24 shows the average amplitudes of the elicited SSVEP of all volunteers for the three visual stimuli. The frequencies marked with an asterisk show statistical significance (p-value < 0.05) using the Friedman test.

At the occipital region, the G-R stimulus showed a higher response when compared with the W stimulus in the medium-frequency range (15–25 Hz, with p-value < 0.05). In contrast, in the high-frequency range (30–40 Hz, p-value < 0.05) the G-B stimulus presented a better response when compared with the W stimulus. In the 55–65 Hz interval, the W stimulus achieved a better response than G-R and G-B stimuli.

In the temporal region (TP9 and TP10), a similar behavior was observed; i.e., in the medium-frequency range, the G-R stimulus achieved higher amplitudes (TP9: 15 Hz,
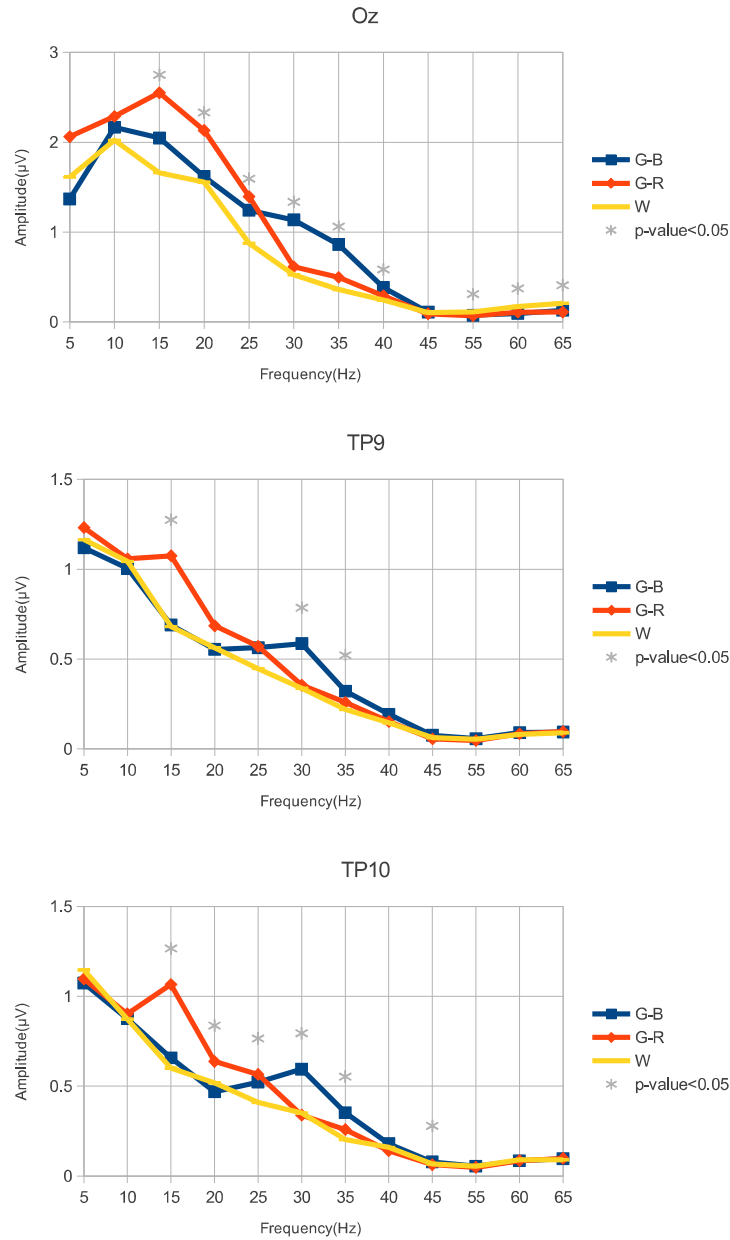
Figure 24 – Average of the steady-state visual evoked potential (SSVEP) amplitudes of all volunteers for the Oz, TP9, and TP10 channels using three different stimuli. The frequencies with statistical significance (p-value $<$ 0.05) based on the Friedman test are marked with an asterisk.

with p-value $<$ 0.05; TP10: 15–25 Hz, with p-value $<$ 0.05) than W and G-B stimuli. In the high-frequency range, the G-B stimulus showed a better response (30–35 Hz, with p-value $<$ 0.05) than the other stimuli.

4.3.2 SNR

Figure 25 shows the average SNR of the SSVEP of all volunteers for the three stimuli. The frequencies marked with an asterisk show statistical significance (p-value $<$

0.05) using the Friedman test.
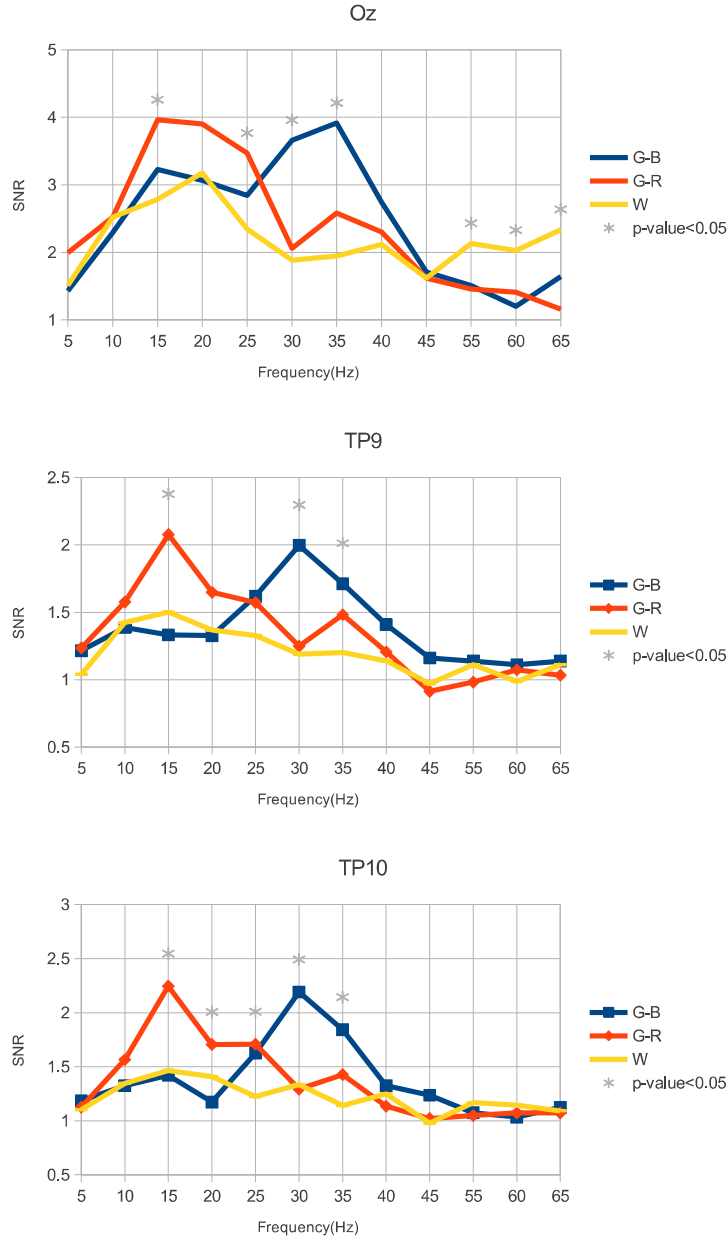
Figure 25 – Average of the SSVEP SNR of all volunteers for the Oz, TP9, and TP10 channels using the three different stimulus configurations. The frequencies with statistical significance (*p*-value < 0.05) based on the Friedman test are marked with an asterisk.

At the occipital region, the G-R stimulus showed a higher response than the W stimulus in the medium-frequency range (15–25 Hz). In the high-frequency range (30–40 Hz), the G-B stimulus showed a better response (30–35 Hz, *p*-value < 0.05) than the W stimulus. In the 55–65 Hz range, the luminance stimulus (W) presented a better response than the G-R and G-B stimuli.

Again, a similar behavior was observed in the temporal region (TP9 and TP10);

i.e., in the medium-frequency range, there was a higher response of the G-R stimulus (TP9: 15 Hz, with p-value < 0.05; TP10: 15–25 Hz, with p-value < 0.05) compared with the luminance stimulus (W). In the high-frequency range the G-B stimulus showed a better response (30–35 Hz, with p-value < 0.05) when compared with the W stimulus.

4.4 Discussion

The literature reports that the visual stimuli that combine colors and luminance can increase the evoked response of P300 potentials (TAKANO et al., 2009; IKEGAMI et al., 2012). Similarly, it was demonstrated that the combination of G-B and luminance can evoke a better response in the SSVEP from the occipital region (BIEGER; MOLINA; ZHU, 2010; AMINAKA; MAKINO; RUTKOWSKI, 2014; SAKURADA et al., 2015). In other work (CHEN et al., 2017), G-R stimuli combined with luminance changes obtained a better response at a modulated frequency of 15 Hz. These works measured the EEG on occipital and parietal regions of the scalp.

Currently, the BCI community is looking at how to transfer these systems from the lab to the patient's home. Thus, more accurate and comfortable BCI systems must be designed. This way, measuring the EEG from hairless positions presents advantages to the user, and recently, these kinds of BCI systems have been reported in the literature (WANG et al., 2015; NORTON et al., 2015; WANG et al., 2017). These studies demonstrated that it is possible to develop a BCI based on EEG measured from hairless regions; however, concerning the wide frequency range and types of stimulation (color and luminance), the question about the best frequency and type of stimulation remains unclear.

In the current study, SSVEP from behind-the-ears areas (TP9 and TP10) was elicited by three stimuli (G-B, G-R, and W) flickering at low-, medium-, and high-frequency. The aim of this experiment was to analyze how these stimuli influence the SSVEP response from the below-the-hairline areas. Higher amplitude (Figure 24) and SNR (Figure 25) of the SSVEP were observed when stimuli that combined color and luminance (G-R and G-B) were applied. Particularly, the best response in the medium-frequency band (15–25 Hz) was obtained with G-R stimulation. On the other hand, G-B stimulation showed the best response in the high-frequency range (30–40 Hz). Therefore, a suitable color and luminance stimulation allows the achievement of higher amplitudes and higher SNR from behind-the-ears areas, and consequently, an accurate and comfortable BCI may be designed.

5 Comparison of Methods for High-Frequency SSVEP-based BCI

Towards more practical systems, calibration-less methods have been used in SSVEP-based BCIs, which have gained attention from researchers, as the detection of the command is performed without a calibration phase for the user. Thus, in the last years, new methods have been developed to improve the SSVEP detection performance. The challenge with high-frequency range is due to its lower signal magnitude, which can degrade the accuracy of the BCI. Thus, this chapter presents a comparison of different techniques for detection of high-frequency SSVEPs. For performance evaluation, classification accuracy and information transfer rate (ITR) were used.

5.1 Introduction

Low- and medium-frequency visual stimuli evoke responses of high magnitude and signal-to-noise ratio (SNR) (ZHU et al., 2010). Consequently, these frequency ranges are most commonly used in SSVEP-based BCIs (VOLOSYAK et al., 2011). However, visual stimulation in these frequency ranges can cause visual fatigue, headaches or photosensitive epileptic seizures (ZHU et al., 2010). On the other hand, the risk of these problems can be reduced using high-frequency visual stimuli. However, the amplitude of SSVEPs is strongly reduced at high-frequency (VOLOSYAK et al., 2011). Thus, robust algorithms are required for the recognition of high-frequency SSVEPs.

One the most traditional method applied for SSVEP detection is the Power Spectral Density Analysis (PSDA)(WANG et al., 2006; WANG et al., 2008). The spectrum of the EEG signal captured can be estimated using the Fast Fourier Transform (FFT) with low computational cost. With advances in EEG signal processing research, other methods for SSVEP detection were developed, such as Canonical Correlation Analysis (CCA) (LIN et al., 2007).

Recently, other techniques, such as Filter Bank Canonical Correlation Analysis (FBCCA) (CHEN et al., 2015a), Multivariate Synchronization Index (MSI) (ZHANG et al., 2014) and Temporally Local Multivariate Synchronization Index (TMSI) (ZHANG et al., 2016) were also developed to improve the SSVEP response detection. These techniques are interesting because the detection of the command is performed without a calibration phase for the user. Thus, the preparation time required for BCI use is reduced, allowing the development of a more practical system.

However, the performance of these techniques for detection of high-frequency SSVEPs in the literature is still unclear. Thus, this evaluation aims to perform a comparison of calibration-less methods for high-frequency SSVEP detection. In addition, medium-frequency range is also analyzed. The classification accuracy and information transfer rate (ITR) index are used for performance evaluation of the methods.

5.2   EEG Signals

Aiming to provide an overview of how the different SNR of SSVEP would impact the design of a future BCI system, a simulated online analysis was performed. Hence, the accuracy of the SSVEP detection and information transfer rate (ITR) (VIALATTE et al., 2010) were used. The dataset used in this analysis was obtained from stimuli evaluation experiment (Chapter 4). To emulate an online detection process, window lengths (WLs) of 1, 2, 3 and 4 s were used. For this test, two frequencies were chosen in order to simulate a binary BCI. Thus, 30 and 35 Hz were chosen for the high-frequency range, as these frequencies presented the best SNR (Figure 25).

5.3   Methods

Researchers have developed various techniques of feature extraction and classification of SSVEPs, such as Power Spectral Density Analysis (PSDA) (WANG et al., 2006), Canonical Correlation Analysis (CCA) (LIN et al., 2007), Filter Bank Canonical Correlation Analysis (FBCCA) (CHEN et al., 2015a), Multivariate Synchronization Index (MSI) (ZHANG et al., 2014), Temporally Local Multivariate Synchronization Index (TMSI) (ZHANG et al., 2016) (Appendix A). The traditional metrics for BCI evaluation are classification accuracy and Information Transfer Rate (ITR) were used (VIALATTE et al., 2010).

5.4   Results and Discussion

Figures 26 and 27 present the average accuracy of the classification of all volunteers for the three stimuli in high-frequency range for occipital and behind-the-ears channels respectively.

Figures 28 and 29 present the average ITR of all volunteers for the three stimuli in high-frequency range for occipital and behind-the-ears channels respectively.

The high-frequency band is known for its low-amplitude SSVEP, making difficult to implement a BCI (VOLOSYAK et al., 2011). However, when using G-B stimuli, the detection accuracy and ITR were increased on both the occipital and temporal areas. The
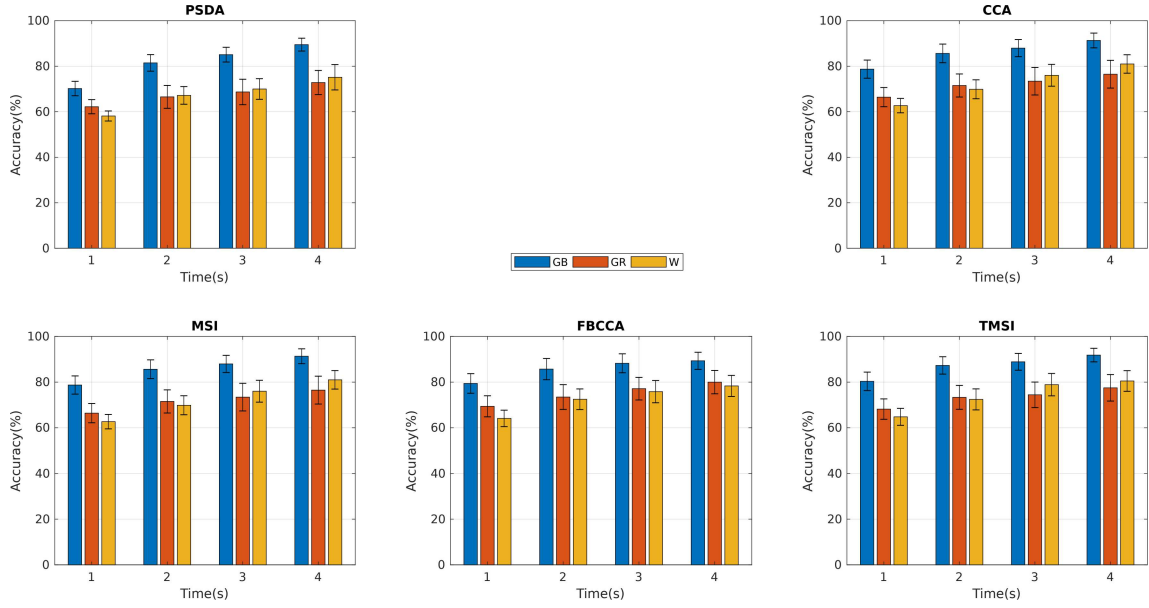
Figure 26 – Average accuracy of all volunteers for the three stimuli in high-frequency range for occipital channel
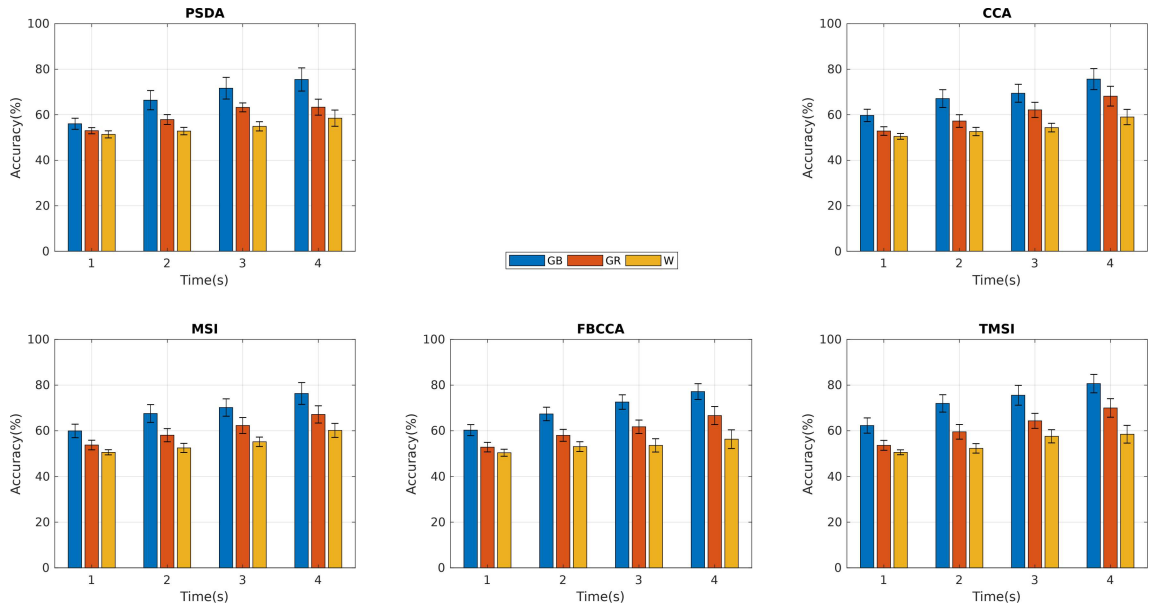
Figure 27 – Average accuracy of all volunteers for the three stimuli in high-frequency range for behind-the-ears channels.

G-B stimulus presented the higher accuracy when compared with G-R and W stimuli using PSDA (TP9/TP10: $75.5 \pm 5.1\%$), CCA (TP9/TP10: $75.7 \pm 4.6\%$), MSI (TP9/TP10: $76.3 \pm 4.8\%$), FBCCA (TP9/TP10: $77.2 \pm 3.5\%$) and TMSI (TP9/TP10: $80.7 \pm 4.2\%$).

In the current evaluation, it is shown that using G-B stimulus at high frequencies allowed a satisfactory accuracy rate to be obtained in a hairless area ($> 80\%$). Hence, the development of more comfortable and practical BCIs are possible. In addition, a previous work (PARRA et al., 2007) reports that the green-blue chromatic flicker is the safest stimulus for human visual photosensitivity.
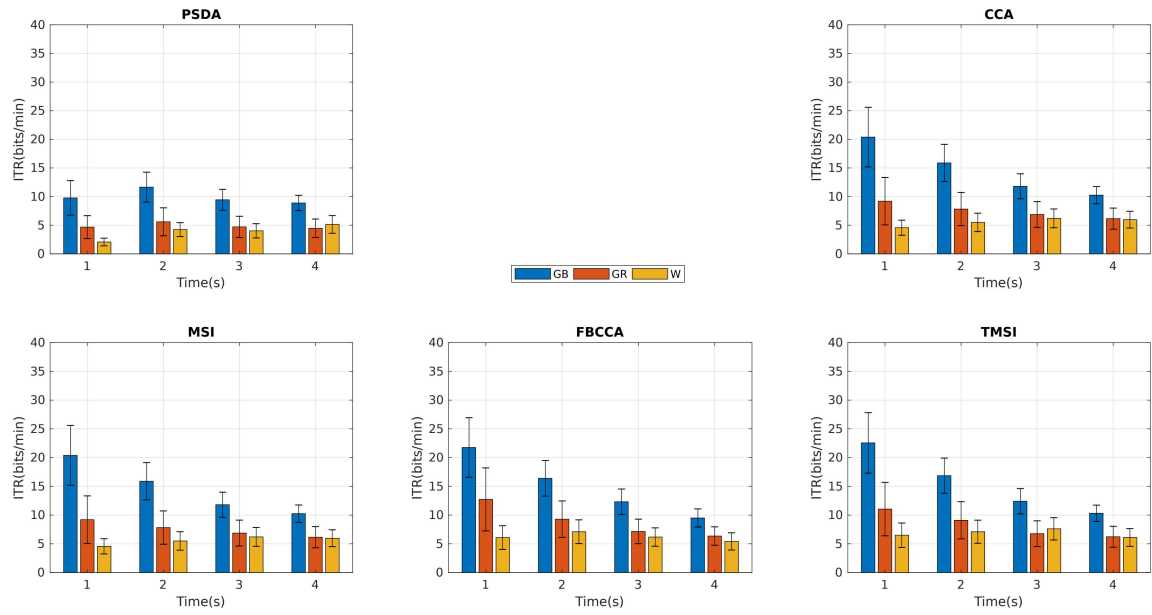
Figure 28 – Average ITR of all volunteers for the three stimuli in high-frequency range for occipital channel.
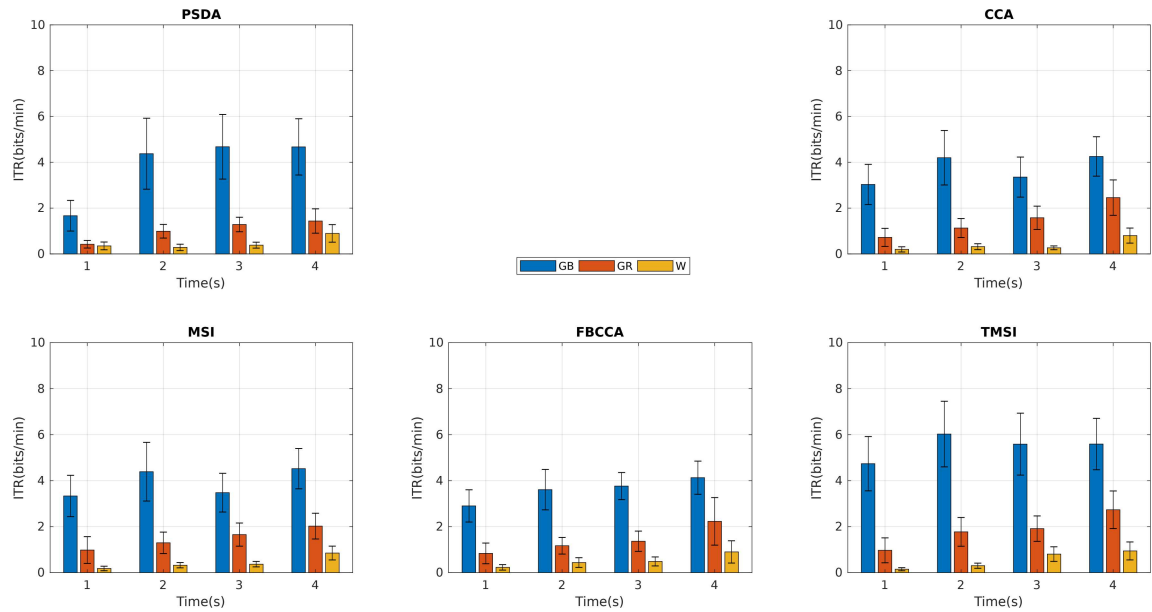
Figure 29 – Average ITR of all volunteers for the three stimuli in high-frequency range for behind-the-ears channels.

6 A Noninvasive High-Frequency SSVEP-based BCI

This chapter presents the development of our Brain-Computer Interface, which is able to modulate the high-frequency SSVEP amplitude from below-the-hairline areas by adjusting the eyes focus. This BCI was validated through the control of a mobile robot in an virtual reality environment.

6.1 Introduction

As previously described, one of the most common BCI paradigms is based on SSVEP (ZHU et al., 2010; VIALATTE et al., 2010). The main advantage of this paradigm is given by its robustness due to the high signal-to-noise ratio (SNR) response (ALLISON et al., 2010; VIALATTE et al., 2010). In SSVEP-based BCIs, each command can be codified with a visual stimulus at a specific frequency (MIDDENDORF et al., 2000; XING et al., 2018). Thus, BCI users are able to send commands to the computer by redirecting their gazing to the target stimulus location (Figure 30) (BASTOS-FILHO et al., 2014).
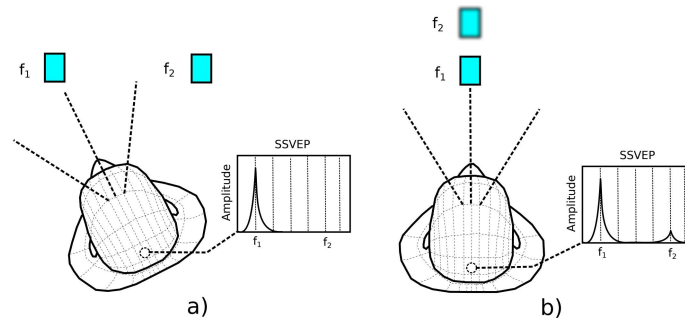
Figure 30 – (a) Illustration of Conventional SSVEP-based BCI; (b) Alternative SSVEP-based BCI stimuli setup with Depth-of-Field.

However, paralyzed individuals who cannot control their muscular movements will have difficulties using these conventional SSVEP-based BCIs. In order to reduce the voluntary movements, alternative SSVEP-based BCIs using two stimuli superimposed or close to each other have been proposed (KELLY et al., 2005; ALLISON et al., 2008; ZHANG et al., 2010; LESENFANTS et al., 2014; TELLO et al., 2016). However, neural competition in virtual cortex increases as the visual stimuli become close (FUCHS et al., 2008), implying a classification accuracy reduction (NG; BRADLEY; CUNNINGTON, 2012; ZHANG et al., 2019). Thus, to obtain a better BCI performance, center-to-center spatial distance between visual stimuli should be more than 6° (ZHANG et al., 2019).

Cotrina et al. (2017) proposed a SSVEP-based BCI composed of two low-frequency stimuli based on Depth-of-Field aiming at reducing the visual stimuli competition as well as required movements. When human eye focuses on an object, the range of distance for which objects produce acceptably sharp retinal image is known Depth-of-Field (PENTLAND, 1987), whereas objects positioned out of this range appear blurred. Thus, users were able to select one of them by shifting their eye focus (COTRINA et al., 2017) (Figure 30). In that work, EEG signals were collected through electrodes placed on occipital and parietal regions (hair-covered areas), which demanded a long preparation time to place the electrodes and dirty the hair with gel(WANG et al., 2012). In addition, generally people with severe motor disabilities need to stay with their heads supported by a headrest, which makes it difficult to use kind of BCIs in everyday life.

Research works about below-the-hairline areas and high-frequency visual stimuli for BCIs have been few explored in the literature, despite this configuration being secure, practical and comfortable for people suffering severe motor disabilities. The reason is because the amplitude of SSVEPs is quite reduced at high-frequency, making it difficult to implement a BCI (VOLOSYAK et al., 2011).

Nevertheless, recently we have shown that chromatic and luminance stimuli allow the achievement of higher amplitudes and higher SNR from behind-the-ears areas. Particularly, for high-frequency range (30-40 Hz), the best response was obtained in green-blue stimulation (Chapter 4). Therefore, it is reasonable to believe that one could use high-frequency SSVEPs from behind-the-ears to implement a SSVEP-based BCI based on Depth-of-Field. Furthermore, to our best knowledge, no study has yet used high-frequency SSVEPs from hairless areas to develop a online system, such as the proposed here.

Thus, this study aims to answer three main questions: (1) Can high-frequency SSVEP measured from below-the-hairline areas be modulated by shifting eye focus? (2) Can these potentials measured from hairless areas be suitable for BCI usage? (3) What is the system performance for online mode? The article follows with an explanation of the materials and methods used in the evaluation of the system. Lastly, some important aspects of the results are shown and discussed.

6.2   Materials and Methods

6.2.1   Data acquisition

Four subjects (ages 24.0 ± 4; 3 M; 1 F) were recruited to participate in this study. The research was carried out in compliance with Helsinki declaration, and the experiments were performed according to the rules of the ethics committee of UFES/Brazil, under registration number CAAE: 64797816.7.0000.5542. All measurements were noninvasive

and the subjects were free to withdraw at any time without any penalty.

For the BCI development, a clinical EEG signal recording equipment (BrainNet-36) was used. We used EEG channels placed on TP9 and TP10 positions (behind-the-ears areas), with the reference at the forehead (Fpz). The sampling frequency was 200 Hz, and the ground electrode was placed on the left ear.

6.2.2   Virtual Environment

The Virtual Environment was created using the *Unity Game Engine*. The robot and its movements were built in the open source software *Blender 3D*. Furthermore, the textures were created using a free license software *Gimp* (Figure 31).
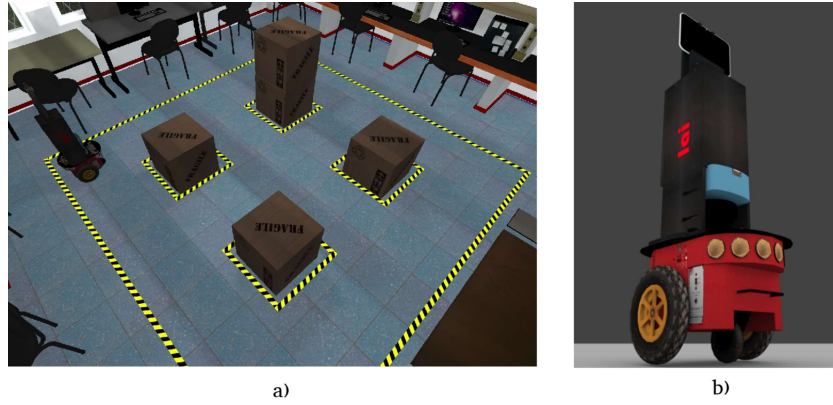
Figure 31 – a)Virtual environment and b) Virtual robot developed.

6.2.3   Stimulus Design

The visual stimulation was performed by two RGB LEDs, and each one illuminated a diffusion board (Figure 32). The signals were generated with the microcontroller ATMega2560 of 16MHz, present in the Arduino Mega 2560 development board, using square waveforms at 31 and 32 Hz. For these experiments, we used the same stimulation setup used in a our previous study. Thus, green-blue stimulus was selected, as this color combination elicited SSVEP with the best SNR in the high-frequency range (Chapter 4).
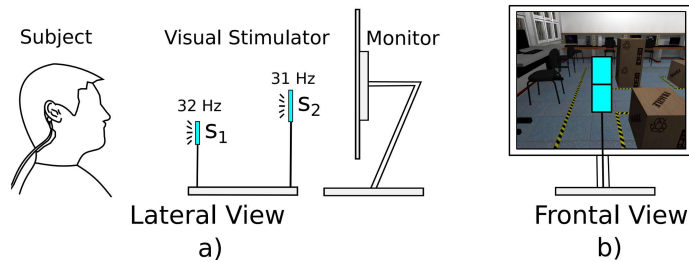
Figure 32 – Layout of the SSVEP-based BCI stimulation setup. a) Lateral View; b) Frontal View.

6.2.4 Signal Processing and Evaluation Protocol

The subjects sat on a comfortable chair 60 cm in front of the stimulation system. The four participants were instructed to perform both offline and online BCI tasks, in which the whole system was properly synchronized.

For the offline protocol, the subject had to focus at each stimulus (S_1 and S_2) for 20 s, and both stimuli were activated. The EEG was preprocessed using a 6th order Butterworth filter with cut-off frequencies set at 3 and 90 Hz. For each recorded channel, the Discrete Fourier Transform (DFT) was applied to the 20-s-long EEG data to calculate the amplitude spectrum $F(f)$ at frequency f. The SNR of the SSVEP at a single channel is defined as the ratio of $F(f)$ to the mean amplitude of the K neighboring frequencies (WANG et al., 2017; WANG et al., 2006):

$$SNR = \frac{K \times F(f)}{\sum_{n=1}^{K/2}[F(f + n\Delta f) + F(f - n\Delta f)]},\qquad(6.1)$$

where Δf is the frequency resolution (0.05 Hz in this study), and $K/2$ was set to 16 (i.e., $\pm$ 0.8 Hz) (CHEN et al., 2014).

The online protocol was performed using a virtual environment (Figure 31) built to simulate the use of the virtual robot (FLORIANO et al., 2016). For this evaluation, three out of four subjects performed the route shown in Figure 33, by sending commands to the virtual robot. The commands implemented in the system were defined as: i) move a meter ahead, which corresponded to the focus on the S_2 stimulus, and ii) rotate 30 degrees to the right when the focus was on the S_1 stimulus (Figure 32).
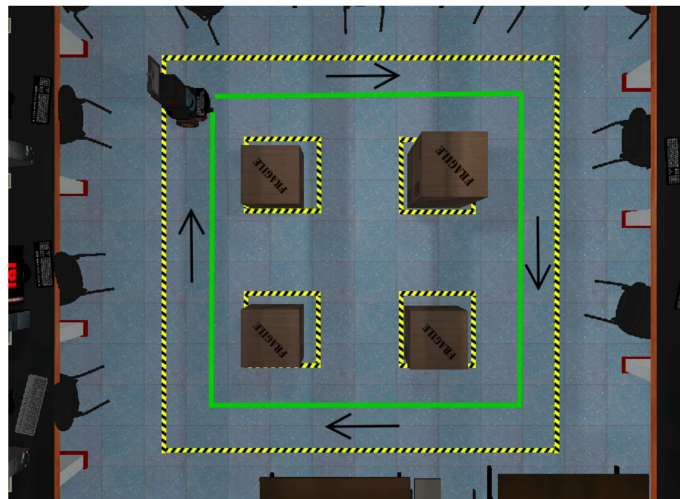
Figure 33 – Task used for online evaluation.

The EEG was analyzed within a time 4 s window, slid in steps of 0.25 s, i.e., the EEG signal processing is performed four times by second. The Temporally Local Multivariate Synchronization Index (TMSI) method (ZHANG et al., 2016) was performed

every 0.25 s using the criterion of maximum value of synchronization index for SSVEP target recognition. Then, in order to send a command, four consecutive targets are classified as the same target, otherwise the acquisition of the signals is resumed. A similar strategy was used in (WANG et al., 2018)

6.3   Results and Discussion

Figure 34 shows the SNR of the SSVEP response elicited by the visual stimuli. The SSVEPs elicited by the visual stimulation setup were consistent and accurate. In both situations (focus on S_1/S_2 stimulus), each spectrum response contains the peak in the expected frequency. In both cases, the peak of the other frequency was absent in the EEG signal spectrum even though both visual stimuli were activated.
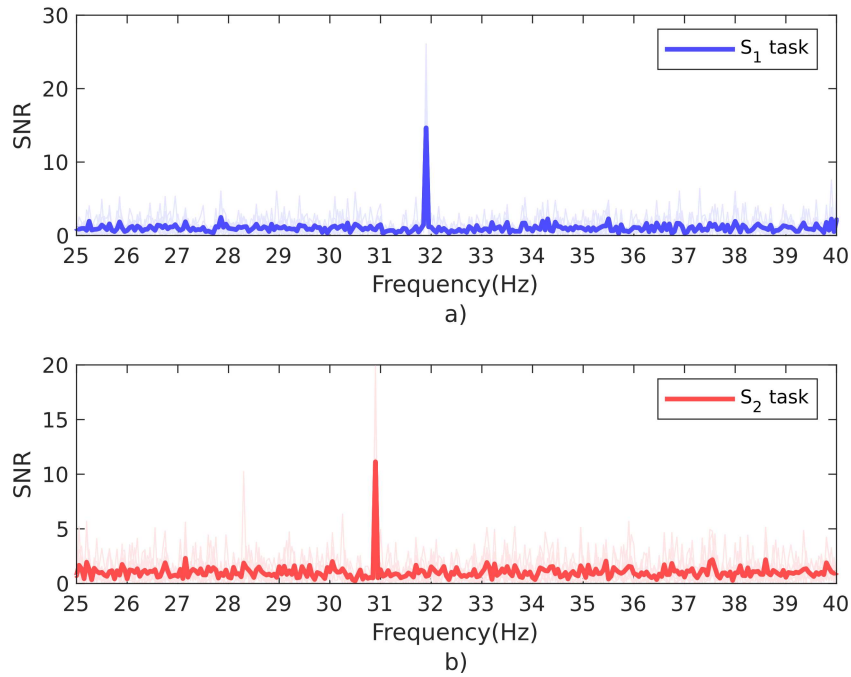
Figure 34 – Average of the SNR SSVEP captured of both EEG channels during the offline protocol performed by all subjects (dark lines) together with SNR corresponding to all trials (bright lines).

Figure 35 shows Synchronization indices calculated with TMSI method using four-second sliding windows (steps of 0.25 s) for the two situations (focus on S_1/S_2 stimulus). The results reveal that the behavior of the SSVEP amplitude was modulated according to the eyes focusing mechanism. For both cases, it can be noticed throughout the trial that the values of the synchronization indices related to the frequency of the focused stimulus is higher than the other one and vice versa.

Figure 36 shows the bars representing the average value of the synchronization indices at frequencies of focused/non-focused stimulus for each subject in the situations:
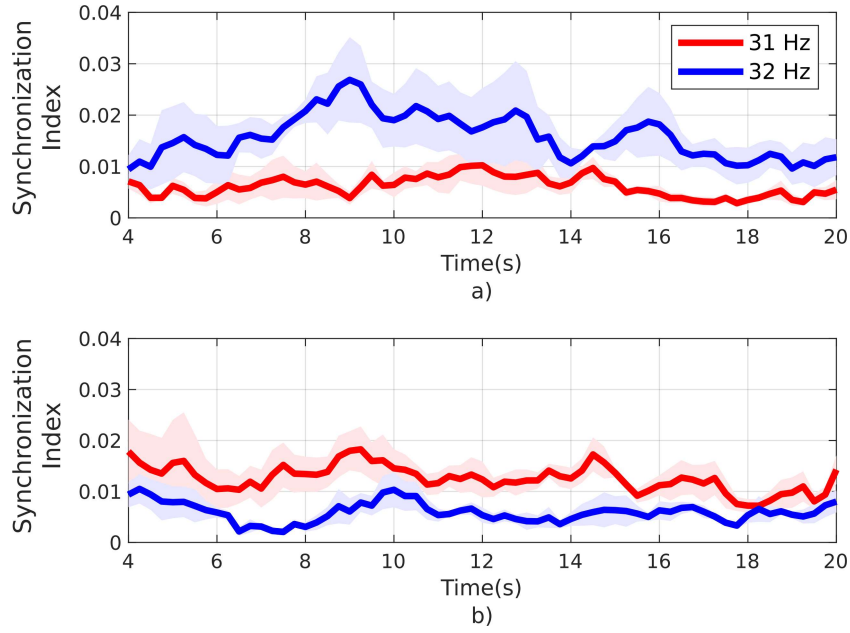
Figure 35 – Synchronization indices of the TMSI method corresponding to the average (dark lines) together with standard error (bright lines). a) The focus was on the S_1 stimulus. b) The focus was on the S_2 stimulus.

a) focus on S_1, and b) S_2 stimulus. The Wilcoxon signed-rank test was used to evaluate the difference at a level of $p < 0.05$. Then, a statistical significant difference was indicated by an asterisk. Thus, it was observed that the focused stimulus elicited distinguishable SSVEP pattern, independent to non-focused stimulus also present in the field of view.

Figure 37 shows the accuracy rate and ITR of the three subjects. Subject #4 was not able to accomplish the online test. Notice in Figure 36 there was no difference between indices. The subjects that were able to perform the proposed task in the protocol obtained an average accuracy of 96% and ITR of 6.42 bits/min. Based on the results, the proposed BCI is considered suitable to be used, for example, for alternative communication interface, as a satisfactory classification accuracy was achieved. Notice that, according to (KÜBLER; BIRBAUMER, 2008), accuracy above 70% is considered acceptable to achieve effective communication in a BCI with binary choice.

As a discussion, although conventional SSVEP-based BCIs are becoming robust systems, they are still not suitable for all patients, as reliable eye control movements are required in these BCIs. Thus, gaze independent approaches based on the attention has been proposed (KELLY et al., 2005; ZHANG et al., 2010; LESENFANTS et al., 2014; TELLO et al., 2016). Nevertheless, independent approaches demand high mental concentration (POSNER; PETERSEN, 1990). For that reason, Cotrina et al. proposed a setup based on the Depth-of-Field phenomenon that becomes a complementary method to the attention based SSVEP paradigm (COTRINA et al., 2017). Table 3 presents a summary of some characteristics of previous related works, comparing them with our study.
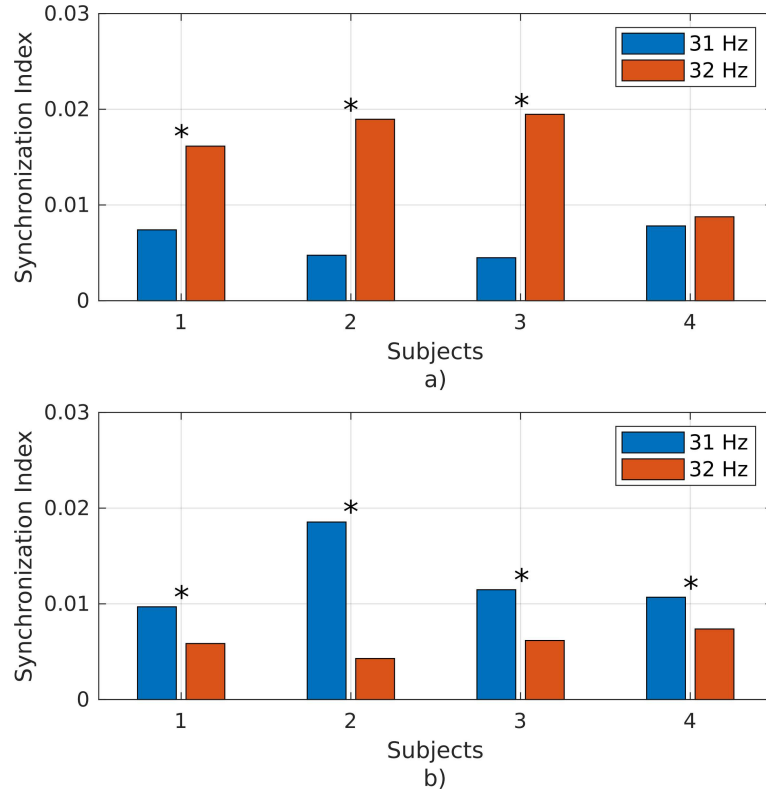
Figure 36 – Average of the synchronization indices of the TMSI method. a) The focus was on the S_1 stimulus. b) The focus was on the S_2 stimulus. The groups with statistical significance (p-value < 0.05) based on the Wilcoxon signed-rank test are marked with an asterisk.
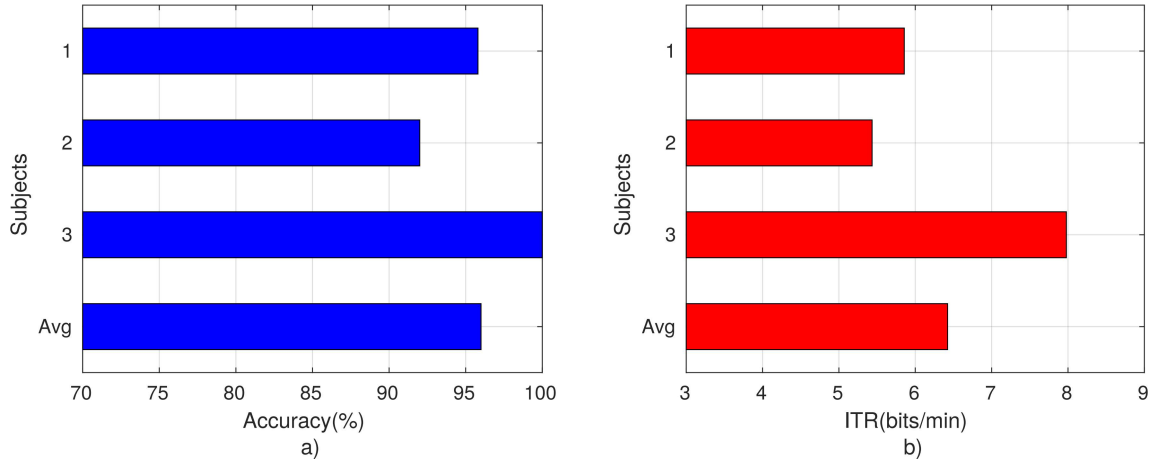
Figure 37 – Results of the online evaluation.

Through the obtained results in our study, it was observed that the high-frequency SSVEP response from hairless regions can also be modulated by focusing mechanism of the eyes. In online evaluation, this response was demonstrated to be suitable for use in a BCI, reaching satisfactory performance using a calibration-less method (accuracy and ITR of 96% and 6.42 bits/min, respectively). Additionally, this system uses comfortable stimuli (high-frequency range), practical electrodes placement and does not require a calibration

phase by users.

Table 3 – Summary of the characteristics of related studies.

Study	Classes	Visual Stimulus	Stimulator Device	High-frequency	Hairless area
(KELLY et al., 2005)	2	Bilateral Squares with Letters	CRT monitor	No	No
(ALLISON et al., 2008)	2	Overlapped Lines	CRT monitor	No	No
(ZHANG et al., 2010)	2	Overlapped Dots	LCD monitor	No	No
(LESENFANTS et al., 2014)	2	Interlaced Squares	LED	No	No
(TELLO et al., 2016)	2	Rubin's Face-Vase	LED	No	No
(COTRINA et al., 2017)	2	Luminance	LED	No	No
This work	2	Chromatic-Luminance	LED	**Yes**	**Yes**

7 Conclusions and Future Works

This thesis presented studies conducted to characterize the SSVEP response from below-the-hairline areas with the aim of developing a practical BCI. Firstly, the results demonstrated that the SSVEP response from hairless areas are influenced by the reference electrode position, and that the best channel choices to measure the response were TP9-Fpz and TP10-Fpz.

Regarding the study about chromatic and luminance visual stimuli, it was found that stimuli based on a suitable color and luminance elicit strong SSVEP on the behind-the-ears areas. Interestingly, it was found a different response of SSVEP related to frequency and color of the stimuli. Thus, although green-red stimulus elicit the highest SSVEP in the medium-frequency range (15–25 Hz), green-blue stimulus elicited the highest SSVEP at high-frequencies (30–40 Hz). Moreover, the results of the simulated online analysis show that a combination of colors and luminance also improve the SSVEP detection accuracy, reaching rates higher than 80% for medium- and high-frequency stimulation.

Another study conducted was about the analysis of the influence of the shifting the eye focus on the SSVEP amplitude in hairless areas. The results demonstrate that it is possible to measure the modulation of the SSVEP amplitude from below-the-hairline areas according to the eye focus, whose SSVEPs elicited by visual stimuli were consistent and accurate. In fact, in both offline tasks (focus on stimulus S_1 and S_2), each response spectrum contained only the peak in the expected frequency. In addition, online results indicated that the proposed BCI can be used for an alternative communication interface, with an average accuracy of 96%. These findings allow the development of more comfortable and practical BCIs with electrodes positioned on below-the-hairline areas.

Future Works

The following are suggestions for future works:

- It is essential a study for creation of a benchmark for a high-frequency SSVEP dataset. This open dataset can be used to compare the performance of new algorithms.

- Development of a low cost wearable BCI system based on this thesis proposal (Figure 38).

- Assessment of the BCI in people with severe motor disabilities such as those in advanced stages of amyotrophic lateral sclerosis and Guillain-Barré syndrome.
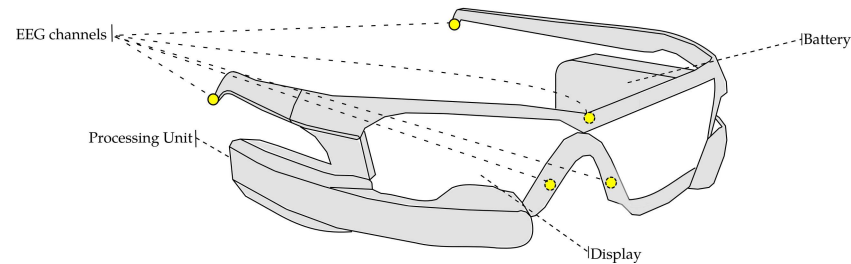
Figure 38 – Design of a low cost wearable BCI system based on this thesis proposal.

Publications

Table 4 present an overview of works developed during the research conducted in this PhD thesis:

Table 4 – Publications

	Published	Under Review
Journal Papers	2 (A1 and B1)	1 (A2)
Conference Papers	6	2
Book Chapters	2	-
Patents	-	2

Bibliography

AKHTAR, A. et al. Playing checkers with your mind: An interactive multiplayer hardware game platform for brain-computer interfaces. In: IEEE. *2014 36th Annual International Conference of the IEEE Engineering in Medicine and Biology Society.* [S.l.], 2014. p. 1650–1653.

ALLISON, B. et al. Bci demographics: How many (and what kinds of) people can use an ssvep bci? *Neural Systems and Rehabilitation Engineering, IEEE Transactions on*, IEEE, v. 18, n. 2, p. 107–116, 2010.

ALLISON, B. Z. et al. Towards an independent brain–computer interface using steady state visual evoked potentials. *Clinical neurophysiology*, Elsevier, v. 119, n. 2, p. 399–408, 2008.

AMINAKA, D.; MAKINO, S.; RUTKOWSKI, T. M. Chromatic ssvep bci paradigm targeting the higher frequency eeg responses. In: IEEE. *Asia-Pacific Signal and Information Processing Association, 2014 Annual Summit and Conference (APSIPA).* [S.l.], 2014. p. 1–7.

ARFKEN, G. B.; WEBER, H. J. *Mathematical methods for physicists.* [S.l.]: AAPT, 1999.

BASTOS-FILHO, T. F. et al. Towards a new modality-independent interface for a robotic wheelchair. *IEEE Transactions on Neural Systems and Rehabilitation Engineering*, IEEE, v. 22, n. 3, p. 567–584, 2014.

BIEGER, J.; MOLINA, G. G.; ZHU, D. Effects of stimulation properties in steady state visual evoked potential based brain-computer interfaces. In: *32nd Annual International Conference of the IEEE Engineering in Medicine and Biology Society.* [S.l.: s.n.], 2010.

BIN, G. et al. An online multi-channel SSVEP-based brain-computer interface using a canonical correlation analysis method. *Journal of neural engineering*, v. 6, n. 4, 2009.

BRIDGERS, S. L.; EBERSOLE, J. S. Eeg outside the hairline detection of epileptiform abnormalities. *Neurology*, AAN Enterprises, v. 38, n. 1, p. 146–146, 1988.

BUBRICK, E. J.; BROMFIELD, E. B.; DWORETZKY, B. A. Utilization of below-the-hairline eeg in detecting subclinical seizures. *Clinical EEG and Neuroscience*, v. 41, n. 1, p. 15–18, 2010.

CAO, L. et al. A hybrid brain computer interface system based on the neurophysiological protocol and brain-actuated switch for wheelchair control. *Journal of neuroscience methods*, Elsevier, v. 229, p. 33–43, 2014.

CHABUDA, A.; DURKA, P.; ŻYGIEREWICZ, J. High frequency ssvep-bci with hardware stimuli control and phase-synchronized comb filter. *IEEE Transactions on Neural Systems and Rehabilitation Engineering*, IEEE, 2017.

CHEN, J. et al. Application of a single-flicker online ssvep bci for spatial navigation. *PloS one*, Public Library of Science, v. 12, n. 5, p. e0178385, 2017.

CHEN, X. et al. A high-itr ssvep-based bci speller. *Brain-Computer Interfaces*, Taylor & Francis, v. 1, n. 3-4, p. 181–191, 2014.

CHEN, X. et al. Filter bank canonical correlation analysis for implementing a high-speed ssvep-based brain–computer interface. *Journal of neural engineering*, IOP Publishing, v. 12, n. 4, p. 046008, 2015.

CHEN, X. et al. High-speed spelling with a noninvasive brain–computer interface. *Proceedings of the National Academy of Sciences*, National Acad Sciences, v. 112, n. 44, p. E6058–E6067, 2015.

CHEN, X. et al. A novel stimulation method for multi-class ssvep-bci using intermodulation frequencies. *Journal of neural engineering*, IOP Publishing, v. 14, n. 2, p. 026013, 2017.

CHENG, M. et al. Design and implementation of a brain-computer interface with high transfer rates. *Biomedical Engineering, IEEE Transactions on*, 2002.

CHUMERIN, N. et al. Steady-state visual evoked potential-based computer gaming on a consumer-grade eeg device. *Computational Intelligence and AI in Games, IEEE Transactions on*, 2013.

CONWAY, B. R.; MOELLER, S.; TSAO, D. Y. Specialized color modules in macaque extrastriate cortex. *Neuron*, Elsevier, v. 56, n. 3, p. 560–573, 2007.

COTRINA, A. et al. A ssvep-bci setup based on depth-of-field. *IEEE Transactions on Neural Systems and Rehabilitation Engineering*, IEEE, v. 25, n. 7, p. 1047–1057, 2017.

DIEZ, P. F. et al. Commanding a robotic wheelchair with a high-frequency steady-state visual evoked potential based brain–computer interface. *Medical engineering & physics*, 2013.

DIEZ, P. F. et al. Asynchronous bci control using high-frequency ssvep. *Journal of neuroengineering and rehabilitation*, BioMed Central, v. 8, n. 1, p. 1, 2011.

FLORIANO, A. et al. Plataforma robótica de telepresencia controlada por señales cerebrales. *Cognitive Area Networks*, p. 9–12, 2016.

FUCHS, S. et al. Attentional bias of competitive interactions in neuronal networks of early visual processing in the human brain. *NeuroImage*, Elsevier, v. 41, n. 3, p. 1086–1101, 2008.

GAO, Q. et al. Controlling of smart home system based on brain-computer interface. *Technology and Health Care*, IOS Press, n. Preprint, p. 1–15, 2018.

GOODALE, M. A.; MILNER, A. D. Separate visual pathways for perception and action. *Trends in neurosciences*, Elsevier, v. 15, n. 1, p. 20–25, 1992.

GRAIMANN, B.; ALLISON, B.; PFURTSCHELLER, G. Brain–computer interfaces: A gentle introduction. In: *Brain-Computer Interfaces*. [S.l.]: Springer, 2010.

GRAIMANN, B.; ALLISON, B.; PFURTSCHELLER, G. Revolutionizing human-computer interaction. In: _____. [S.l.]: Springer-Verlag, 2010. cap. Brain-Computer Interface: A Gentle Introduction, p. 1–28.

GUGER, C. et al. How many people could use an SSVEP BCI? *Frontiers in neuroscience*, v. 6, 2012.

GUYTON, A.; HALL, J. Textbook of medical physiology 11th edition elsevier inc. *Philadelphia PA*, 2006.

HE, B. et al. Brain-computer interfaces. In: _____. *Neural Engineering*. USA: Springer, 2013. p. 87–151.

HERRMANN, C. Human EEG responses to 1-100 hz flicker: resonance phenomena in visual cortex and their potential correlation to cognitive phenomena. *Experimental brain research*, v. 137, n. 3-4, p. 346–353, 2001.

HSU, H.-T. et al. Evaluate the feasibility of using frontal ssvep to implement an ssvep-based bci in young, elderly and als groups. IEEE, 2016.

HWANG, H.-J. et al. Development of an ssvep-based bci spelling system adopting a qwerty-style led keyboard. *Journal of neuroscience methods*, Elsevier, v. 208, n. 1, p. 59–65, 2012.

IKEGAMI, S. et al. Effect of the green/blue flicker matrix for p300-based brain–computer interface: an eeg–fmri study. *Frontiers in neurology*, Frontiers, v. 3, p. 113, 2012.

JUKIEWICZ, M.; CYSEWSKA-SOBUSIAK, A. Stimuli design for ssvep-based brain computer-interface. *International Journal of Electronics and Telecommunications*, v. 62, n. 2, p. 109–113, 2016.

JURCAK, V.; TSUZUKI, D.; DAN, I. 10/20, 10/10, and 10/5 systems revisited: their validity as relative head-surface-based positioning systems. *Neuroimage*, Elsevier, v. 34, n. 4, p. 1600–1611, 2007.

KANDEL, E. R. et al. *Principles of neural science*. [S.l.]: McGraw-Hill New York, 2013.

KELLY, S. P. et al. Visual spatial attention control in an independent brain-computer interface. *IEEE Transactions on Biomedical Engineering*, IEEE, v. 52, n. 9, p. 1588–1596, 2005.

KOIDA, K.; KOMATSU, H. Effects of task demands on the responses of color-selective neurons in the inferior temporal cortex. *Nature neuroscience*, Nature Publishing Group, v. 10, n. 1, p. 108–116, 2007.

KÜBLER, A.; BIRBAUMER, N. Brain–computer interfaces and communication in paralysis: extinction of goal directed thinking in completely paralysed patients? *Clinical neurophysiology*, Elsevier, v. 119, n. 11, p. 2658–2666, 2008.

KWAK, N.-S.; MÜLLER, K.-R.; LEE, S.-W. A lower limb exoskeleton control system based on steady state visual evoked potentials. *Journal of neural engineering*, IOP Publishing, v. 12, n. 5, p. 056009, 2015.

LALOR, E. C. et al. Steady-state vep-based brain-computer interface control in an immersive 3d gaming environment. *EURASIP journal on applied signal processing*, 2005.

LEGENY, J.; VICIANA-ABAD, R.; LECUYER, A. Toward contextual ssvep-based bci controller: smart activation of stimuli and control weighting. *IEEE transactions on Computational Intelligence and AI in Games*, IEEE, v. 5, n. 2, p. 111–116, 2013.

LESENFANTS, D. et al. An independent ssvep-based brain–computer interface in locked-in syndrome. *Journal of neural engineering*, IOP Publishing, v. 11, n. 3, p. 035002, 2014.

LIN, Z. et al. Frequency recognition based on canonical correlation analysis for ssvep-based bcis. *IEEE Transactions on Biomedical Engineering*, IEEE, v. 54, n. 6, p. 1172–1176, 2007.

LIU, Q. et al. Review: Recent development of signal processing algorithms for ssvep-based brain computer interfaces. *Journal of Medical and Biological Engineering*, 2013.

MARTIŠIUS, I.; DAMAŠEVIČIUS, R. A prototype ssvep based real time bci gaming system. *Computational intelligence and neuroscience*, Hindawi Publishing Corp., v. 2016, p. 18, 2016.

MIDDENDORF, M. et al. Brain-computer interfaces based on the steady-state visual-evoked response. *IEEE transactions on rehabilitation engineering : a publication of the IEEE Engineering in Medicine and Biology Society*, v. 8, n. 2, p. 211–214, 2000.

MISHKIN, M.; UNGERLEIDER, L. G. Contribution of striate inputs to the visuospatial functions of parieto-preoccipital cortex in monkeys. *Behavioural brain research*, Elsevier, v. 6, n. 1, p. 57–77, 1982.

MORA, N.; MUNARI, I. D.; CIAMPOLINI, P. A multi-modal bci system for active and assisted living. In: SPRINGER. *International Conference on Smart Homes and Health Telematics*. [S.l.], 2016. p. 345–355.

MULERT, C.; LEMIEUX, L. *EEG-fMRI: physiological basis, technique, and applications.* [S.l.]: Springer Science & Business Media, 2009.

MULLER-PUTZ, G. R.; PFURTSCHELLER, G. Control of an electrical prosthesis with an ssvep-based bci. *IEEE Transactions on biomedical engineering*, IEEE, v. 55, n. 1, p. 361–364, 2008.

MÜLLER, S. M. T.; BASTOS, T. F.; SARCINELLI, M. Proposal of a ssvep-bci to command a robotic wheelchair. *Journal of Control, Automation and Electrical Systems*, Springer, v. 24, n. 1-2, p. 97–105, 2013.

NAKANISHI, M. et al. A high-speed brain speller using steady-state visual evoked potentials. *International journal of neural systems*, World Scientific, v. 24, n. 06, p. 1450019, 2014.

NG, K. B.; BRADLEY, A. P.; CUNNINGTON, R. Stimulus specificity of a steady-state visual-evoked potential-based brain–computer interface. *Journal of Neural engineering*, IOP Publishing, v. 9, n. 3, p. 036008, 2012.

NICOLAS-ALONSO, L. F.; GOMEZ-GIL, J. Brain computer interfaces, a review. *Sensors*, Basel, v. 12, n. 2, p. 1211–1279, 2012.

NORCIA, A. M. et al. The steady-state visual evoked potential in vision research: A review. *Journal of Vision*, The Association for Research in Vision and Ophthalmology, v. 15, n. 6, p. 4–4, 2015.

NORTON, J. J. et al. Soft, curved electrode systems capable of integration on the auricle as a persistent brain–computer interface. *Proceedings of the National Academy of Sciences*, National Acad Sciences, v. 112, n. 13, p. 3920–3925, 2015.

ODOM, J. V. et al. Visual evoked potentials standard (2004). *Documenta ophthalmologica*, 2004.

ORTNER, R. et al. An SSVEP BCI to control a hand orthosis for persons with tetraplegia. *IEEE transactions on neural systems and rehabilitation engineering : a publication of the IEEE Engineering in Medicine and Biology Society*, v. 19, n. 1, p. 1–5, 2011.

PARRA, J. et al. Is colour modulation an independent factor in human visual photosensitivity? *Brain*, Oxford University Press, v. 130, n. 6, p. 1679–1689, 2007.

PASTOR, M. A. et al. Human cerebral activation during steady-state visual-evoked responses. *The journal of neuroscience*, Soc Neuroscience, v. 23, n. 37, p. 11621–11627, 2003.

PENTLAND, A. P. A new sense for depth of field. *IEEE transactions on pattern analysis and machine intelligence*, IEEE, n. 4, p. 523–531, 1987.

PFURTSCHELLER, G. et al. Self-paced operation of an SSVEP-Based orthosis with and without an imagery-based "brain switch:" a feasibility study towards a hybrid BCI. *IEEE transactions on neural systems and rehabilitation engineering : a publication of the IEEE Engineering in Medicine and Biology Society*, v. 18, n. 4, p. 409–414, 2010.

POSNER, M. I.; PETERSEN, S. E. The attention system of the human brain. *Annual review of neuroscience*, Annual Reviews 4139 El Camino Way, PO Box 10139, Palo Alto, CA 94303-0139, USA, v. 13, n. 1, p. 25–42, 1990.

PUCE, A.; HÄMÄLÄINEN, M. A review of issues related to data acquisition and analysis in eeg/meg studies. *Brain sciences*, Multidisciplinary Digital Publishing Institute, v. 7, n. 6, p. 58, 2017.

PUNSAWAD, Y.; WONGSAWAT, Y. Minimal-assisted ssvep-based brain-computer interface device. In: IEEE. *Proceedings of The 2012 Asia Pacific Signal and Information Processing Association Annual Summit and Conference*. [S.l.], 2012. p. 1–4.

RAMADAN, R. A.; VASILAKOS, A. V. Brain computer interface: control signals review. *Neurocomputing*, Elsevier, v. 223, p. 26–44, 2017.

RAMOS, S. G. et al. Experimental evidences for visual evoked potentials with stimuli beyond the conscious perception threshold. In: IEEE. *ISSNIP Biosignals and Biorobotics Conference 2011*. [S.l.], 2011. p. 1–5.

REGAN, D. *Human brain electrophysiology: evoked potentials and evoked magnetic fields in science and medicine*. [S.l.]: Elsevier, 1989.

SAKURADA, T. et al. Use of high-frequency visual stimuli above the critical flicker frequency in a ssvep-based bmi. *Clinical Neurophysiology*, Elsevier, v. 126, n. 10, p. 1972–1978, 2015.

SAKURADA, T. et al. A bmi-based occupational therapy assist suit: asynchronous control by ssvep. *Frontiers in neuroscience*, Frontiers, v. 7, p. 172, 2013.

SAVIĆ, A.; KISIĆ, U.; POPOVIĆ, M. Toward a hybrid bci for grasp rehabilitation. In: SPRINGER. *5th European Conference of the International Federation for Medical and Biological Engineering.* [S.l.], 2011. p. 806–809.

SHERWOOD, L. *Human physiology: from cells to systems.* [S.l.]: Cengage learning, 2015.

SHYU, K.-K. et al. Development of a low-cost fpga-based ssvep bci multimedia control system. *IEEE Transactions on biomedical circuits and systems*, IEEE, v. 4, n. 2, p. 125–132, 2010.

TAKANO, K. et al. Visual stimuli for the p300 brain-computer interface: a comparison of white/gray and green/blue flicker matrices. *Clinical neurophysiology*, Elsevier, v. 120, n. 8, p. 1562–1566, 2009.

TELLO, R. J. M. G. et al. Development of a human machine interface for control of robotic wheelchair and smart environment. In: *11th IFAC Symposium on Robot Control (SYROCO).* [S.l.: s.n.], 2015.

TELLO, R. M. et al. An independent-bci based on ssvep using figure-ground perception (fgp). *Biomedical Signal Processing and Control*, Elsevier, v. 26, p. 69–79, 2016.

VIALATTE, F.-B. et al. Steady-state visually evoked potentials: focus on essential paradigms and future perspectives. *Progress in neurobiology*, Elsevier, v. 90, n. 4, p. 418–438, 2010.

VOLOSYAK, I. et al. Evaluation of the bremen ssvep based bci in real world conditions. In: IEEE. *Rehabilitation Robotics, 2009. ICORR 2009. IEEE International Conference on.* [S.l.], 2009. p. 322–331.

VOLOSYAK, I. et al. Bci demographics ii: how many (and what kinds of) people can use a high-frequency ssvep bci? *Neural Systems and Rehabilitation Engineering, IEEE Transactions on*, IEEE, v. 19, n. 3, p. 232–239, 2011.

WANG, M. et al. A wearable ssvep-based bci system for quadcopter control using head-mounted device. *IEEE Access*, IEEE, v. 6, p. 26789–26798, 2018.

WANG, Y. et al. Brain-computer interfaces based on visual evoked potentials. *Engineering in Medicine and Biology Magazine, IEEE*, IEEE, v. 27, n. 5, p. 64–71, 2008.

WANG, Y. et al. A practical vep-based brain-computer interface. *Neural Systems and Rehabilitation Engineering, IEEE Transactions on*, 2006.

WANG, Y.-T. et al. Developing an online steady-state visual evoked potential-based brain-computer interface system using eareeg. In: IEEE. *Engineering in Medicine and Biology Society (EMBC), 2015 37th Annual International Conference of the IEEE.* [S.l.], 2015. p. 2271–2274.

WANG, Y.-T. et al. An online brain-computer interface based on ssveps measured from non-hair-bearing areas. *IEEE Transactions on Neural Systems and Rehabilitation Engineering*, IEEE, v. 25, n. 1, p. 14–21, 2017.

WANG, Y.-T. et al. Measuring steady-state visual evoked potentials from non-hair-bearing areas. In: IEEE. *Engineering in Medicine and Biology Society (EMBC), 2012 Annual International Conference of the IEEE.* [S.l.], 2012. p. 1806–1809.

WEI, C.-S. et al. Toward non-hair-bearing brain-computer interfaces for neurocognitive lapse detection. In: IEEE. *Engineering in Medicine and Biology Society (EMBC), 2015 37th Annual International Conference of the IEEE.* [S.l.], 2015. p. 6638–6641.

WOLPAW, J. et al. Brain-computer interfaces for communication and control. *Clinical neurophysiology : official journal of the International Federation of Clinical Neurophysiology*, v. 113, n. 6, p. 767–791, 2002.

WON, D.-O. et al. Effect of higher frequency on the classification of steady-state visual evoked potentials. *Journal of neural engineering*, IOP Publishing, v. 13, n. 1, p. 016014, 2015.

WU, C.-H. et al. Frequency recognition in an ssvep-based brain computer interface using empirical mode decomposition and refined generalized zero-crossing. *Journal of neuroscience methods*, Elsevier, v. 196, n. 1, p. 170–181, 2011.

XIE, S.; MENG, W. Ssvep-based bci for lower limb rehabilitation. In: *Biomechatronics in Medical Rehabilitation.* [S.l.]: Springer, 2017. p. 69–86.

XING, X. et al. A high-speed ssvep-based bci using dry eeg electrodes. *Scientific reports*, Nature Publishing Group, v. 8, n. 1, p. 14708, 2018.

XU, Z. et al. Steady-state visually evoked potential (ssvep)-based brain-computer interface (bci): a low-delayed asynchronous wheelchair control system. In: SPRINGER. *International Conference on Neural Information Processing.* [S.l.], 2012. p. 305–314.

YIJUN, W. et al. Brain-computer interface based on the high-frequency steady-state visual evoked potential. In: IEEE. *Neural Interface and Control, 2005. Proceedings. 2005 First International Conference on.* [S.l.], 2005. p. 37–39.

YIN, E. et al. A dynamically optimized ssvep brain–computer interface (bci) speller. *IEEE Transactions on Biomedical Engineering*, IEEE, v. 62, n. 6, p. 1447–1456, 2014.

YOUNG, G. B. et al. Seizure detection with a commercially available bedside eeg monitor and the subhairline montage. *Neurocritical care*, Springer, v. 11, n. 3, p. 411, 2009.

ZENG, X. et al. A feasibility study of ssvep-based passive training on an ankle rehabilitation robot. *Journal of Healthcare Engineering*, Hindawi, v. 2017, 2017.

ZHANG, D. et al. An independent brain–computer interface using covert non-spatial visual selective attention. *Journal of neural engineering*, IOP Publishing, v. 7, n. 1, p. 016010, 2010.

ZHANG, N. et al. Retinotopic and topographic analyses with gaze restriction for steady-state visual evoked potentials. *Scientific reports*, Nature Publishing Group, v. 9, n. 1, p. 4472, 2019.

ZHANG, Y. et al. Robust frequency recognition for ssvep-based bci with temporally local multivariate synchronization index. *Cognitive neurodynamics*, Springer, v. 10, n. 6, p. 505–511, 2016.

ZHANG, Y. et al. Multivariate synchronization index for frequency recognition of ssvep-based brain–computer interface. *Journal of neuroscience methods*, Elsevier, v. 221, p. 32–40, 2014.

ZHAO, X. et al. Ssvep-based brain–computer interface controlled functional electrical stimulation system for upper extremity rehabilitation. *IEEE Transactions on Systems, Man, and Cybernetics: Systems*, IEEE, v. 46, n. 7, p. 947–956, 2016.

ZHU, D. et al. A survey of stimulation methods used in ssvep-based bcis. *Computational intelligence and neuroscience*, Hindawi Publishing Corp., v. 2010, p. 1, 2010.

Appendix

APPENDIX A − Calibration-less methods for SSVEP detection

A.1 Methods

A.1.1 Power Spectral Density Analysis (PSDA)

Power Spectral Density Analysis (PSDA) is a traditional method used for SSVEP classification (LIU et al., 2013). Fast Fourier Transform (FFT) have been used to estimate the power values at the frequencies of interest for SSVEP detection (WANG et al., 2006; WANG et al., 2008). Thus, a large power amplitude is expected at frequency components corresponding to the fundamental frequency of the stimulus and its harmonics, representing the SSVEP. Furthermore, in PSDA method the SSVEP response can be enhanced for detection by computing the the Equation A.1 based on the SNR as (WANG et al., 2006):

$$SNR(f_i) = \frac{K \times F(f_i)}{\sum_{n=1}^{K/2}[F(f_i + n\Delta f) + F(f_i - n\Delta f)]},\tag{A.1}$$

where f_i is the frequency value, $F(f_i)$ is the magnitude of the signal, Δf is the frequency resolution and K is the number of neighboring frequencies. The frequency with the largest $SNR(f_i)$ is recognized as a BCI command.

A.1.2 Canonical Correlation Analysis (CCA)

CCA is a multi-dimensional statistical analysis technique that finds underlying linear correlations between two sets of data. Given two multi-dimensional data sets X and Y, the CCA finds the weight vectors Wx and Wy that maximize the correlation between linear combinations $x = X^T Wx$ and $y = Y^T Wy$ by solving the following optimization problem:

$$max(p)_{W_x,W_y} = \frac{E[W_x^T XY^T W_y]}{\sqrt{E[W_x^T X X^T W_x]E(W_y^T YY^T W_y)}},\tag{A.2}$$

where $E[.]$ is the expected value.

This problem can be solved using the singular-value decomposition method to diagonalize the covariance matrices as the maximum canonical correlation corresponds to the square-root of the largest eigenvalue.

In SSVEP detection, CCA is used to find linear correlations between multichannel EEG data, X, and a set of reference signals Y_f. This reference set consists of sine and cosine signals at the fundamental and harmonic frequencies of each stimulus.

The reference signal Y_f, shown below, can be derived using N_h harmonics, where f is the fundamental frequency and t is time.

$$Y_f = \begin{pmatrix} sin(2\pi f t) \\ cos(2\pi f t) \\ \vdots \\ sin(2\pi N_h f t) \\ cos(2\pi N_h f t) \end{pmatrix} \tag{A.3}$$

Assume there are K stimulus frequencies to be recognize. It is estimated the canonical correlations indices $p_1, p_2, ..., p_K$ for all of the stimulus frequencies. The stimulus (f_i) that presents the larger value of correlation (p_i) is chosen as the output of the classification.

A.1.3   Multivariate Synchronization Index (MSI)

Zhang et al. (2014) proposed a Multivariate synchronization index (MSI) for frequency recognition. This method calculates the synchronization between multichannel EEGs and the reference signals defined according to the stimulus frequency.

Consider a matrix X of size NxM as the EEG signals and a matrix Y of size $2N_h$xM as the reference signals, where N is the number of channels, M is the number of samples and N_h is the number of harmonics of the reference signal. Assuming both the X and Y have been normalized to have zero means and unit variances. Then the correlation matrix C is

$$C = \begin{bmatrix} C_{11} & C_{12} \\ C_{21} & C_{22} \end{bmatrix} \tag{A.4}$$

Where,

$$\begin{aligned} C_{11} = \tfrac{1}{M}XX^T \quad C_{12} = \tfrac{1}{M}XY^T \\ \\ C_{21} = \tfrac{1}{M}YX^T \quad C_{22} = \tfrac{1}{M}YY^T \end{aligned} \tag{A.5}$$

The matrix C includes the autocorrelation and cross-correlation of X and Y, since autocorrelation influence the synchronization measure the following linear transforming is

applied

$$U = \begin{bmatrix} C_{11}^{-\left(\frac{1}{2}\right)} & 0 \\ 0 & C_{22}^{-\left(\frac{1}{2}\right)} \end{bmatrix} \tag{A.6}$$

$$R = UCU^T = \begin{bmatrix} I_{N \times N} & C_{11}^{-\left(\frac{1}{2}\right)} C_{12} C_{22}^{-\left(\frac{1}{2}\right)} \\ \\ C_{11}^{-\left(\frac{1}{2}\right)} C_{21} C_{22}^{-\left(\frac{1}{2}\right)} & I_{2N_h \times 2N_h} \end{bmatrix} \tag{A.7}$$

Let $\lambda_1, \lambda_2, ..., \lambda_P$ be the eigenvalues of the matrix R, where $P = N + 2N_h$. Then the normalized eigenvalues are given by

$$\lambda_i^n = \frac{\lambda_i}{\sum\limits_{i=1}^{P} \lambda_i} \tag{A.8}$$

Then the S-estimator which represents the synchronization of the signals is defined by

$$S = 1 + \frac{\sum\limits_{i=1}^{P} \lambda_i^n log \lambda_i^n}{log P} \tag{A.9}$$

and varies from 0 which means no correlation and 1 which means maximum correlation. Assume there are K stimulus frequencies to be recognize. Through constructing the reference signal set at each of the stimulus frequency, we estimate the synchronization indices $S_1, S_2, ..., S_K$ for all of the stimulus frequencies. The criterion of maximum value of synchronization indice is used for SSVEP target recognition.

A.1.4 Filter Bank Canonical Correlation Analysis (FBCCA)

Filter Bank Canonical Correlation Analysis (FBCCA) decomposes SSVEPs into multiple sub-band components and then performs separate CCA's on each of the sub-band components (CHEN et al., 2015a). The correlation values between the sub-band components and the reference signal X_k corresponding to f_k stimulation frequency are estimated to form a correlation vector $p_k = [p_k^1, ..., p_k^N]^T$, where N is the number of correlation values. A weighted sum of squares of the correlation values corresponding to all sub-band components is then calculated as the feature for SSVEP detection as follows:

$$P_k = 1 + \sum\limits_{n=1}^{N} w(n)(p_k^n)^2 \tag{A.10}$$

where N is the number of sub-bands and $w(n)$ are the weights of the sub-band components. The weights are set by the observation that the SNR of SSVEP harmonics decreases as the response frequency increases:

$$w(n) = n^{-1.25} + 0.25, n \in [1, N] \tag{A.11}$$

The frequency of the reference signals having the maximum correlation is then considered to be the target stimulus.

A.1.5 Temporally Local Multivariate Synchronization Index (TMSI)

The MSI is a potential method for frequency recognition, however, it is a time dependent method, which is its inconvenience. This method can be improved by integrating the temporal structure information of signals into the covariance matrix. Thus, the time-dependant covariance modelling of the EEG signals can yield more robust features for frequency recognition for SSVEP-based BCI system.

Considering $W \in R^{MxM}$, the weight matrix (or termed adjacency matrix), multivariate signals by $Z = [z_1, z_2, ..., z_M \in R^{NxM}$ respectively. M is the number of recording samples, and N are the number of variables or channels. As stated by Wang, 2010, the temporally local covariance matrix is expressed as shown in Equation A.12:

$$\overline{C} = \frac{1}{2M} \sum_{i=1} M \sum j = 1 M W_{i,j} (z_i - z_j)(z_i - z_j)^T. \tag{A.12}$$

Equation A.13 can be written as:

$$\overline{C} = \frac{1}{M} \sum_{i=1} M (z_i z_j)^T \sum j = 1 M W_{i,j} - \sum_{i=1} M \sum j = 1 M W_{i,j} z_i z_j^T, \tag{A.13}$$

Equation A.13 can be rewritten as:

$$\overline{C} = \frac{1}{M} (Z(D - W)Z^T) = \frac{1}{M} Z L Z^T, \tag{A.14}$$

where L is the Laplacian matrix and $L = D - W \cdot D$ is a diagonal matrix with the diagonal elements being the row sums of W. Different ways can be followed to generate the weight matrix W. Following the Tukeys tricube weighting function, Equation A.15 is reached.

$$W_{i,j} = K \left(\frac{j - i}{\tau} \right). \tag{A.15}$$

Here τ defines the temporally local range, and it features the manifold of the EEG signals. An monotonously decreasing function is used to closed data point that have larger weight between them and it is expressed in Equation A.16

$$K(v) = \begin{cases} (1 - |v|^r)^r, |v| < 1 \\ 0, |v| \geq 1. \end{cases} \tag{A.16}$$

.

Once $\overline{C}$ is generated, to calculate the synchronization index it was used the Equation A.6 - A.9 to implement frequency recongition. Thus, the main operation for the TMSI is to model the covariance matrix $\overline{C}$ which could deliver more discriminative information than its counterpart for the standard MSI.